Next Energy 11 (2026) 100543

Contents lists available at ScienceDirect

Next Energy

journal homepage: www.sciencedirect.com/journal/next-energy

Review article

Comparison of methanol to gasoline (MTG) and methanol to kerosene (MTK) for the decarbonization of the road transport and aviation sectors

Ahtasham Rahim, Giovanni Manente*, Antonio Ficarella

University of Salento, Department of Engineering for Innovation, Lecce, Italy

ARTICLE INFO

Keywords:
Methanol to gasoline
Methanol to kerosene
E-fuels
Process synthesis
Methanol to olefins

ABSTRACT

For the climate goals to be met, it is critical to rapidly increase the share of renewable fuels in the non-electrified road transport sector as well as in the aviation sector. Among the various pathways for renewable fuel production, Methanol-to-Gasoline (MTG) and Methanol-to-Kerosene (MTK) appear particularly promising, especially when considering the continuous decrease of the electrolytic hydrogen production cost and the growing market of e-methanol plants. In this work, a comparative analysis is presented for these 2 pathways, focusing on their process layouts, types of reactors and catalysts, fuel product yields, energy efficiencies, and economics. The MTG pathway is based on a highly selective conversion of methanol into gasoline range hydrocarbons using dimethyl ether as the intermediate, whereas MTK uses a more elaborate cascade of catalytic steps, including methanol-to-olefins, oligomerization, and hydro-processing to produce a high-quality sustainable aviation fuel. The design aspects related to the process layouts and performance optimization are thoroughly examined in order to gain a deeper understanding of the differences between MTG and MTK for a possible facility repurposing as well as to assess any chance for further technology advancements. In considering both these pathways from the perspective of sustainability and energy transition, this review adds to the current research that rarely addresses the connection between these 2 synthetic fuel production technologies.

1. Introduction

The global transportation sector is undergoing a transformative shift driven by the urgent need to reduce greenhouse gas (GHG) emissions and mitigate climate change. The aviation industry, in particular, faces significant challenges due to its reliance on energy-dense liquid fuels, with limited scope for electrification compared to road transport. Both the International Civil Aviation Organization (ICAO) and the International Air Transport Association have set ambitious targets to achieve net-zero CO_2 emissions by 2050, necessitating the rapid development and adoption of sustainable fuel alternatives [1,2]. Simultaneously, the demand for air travel continues to rise, contributing to increasing CO_2 emissions unless effective mitigation strategies are implemented [3]. In the year 2023, the aviation sector contributed for 2.5% to the total CO_2 emissions globally, and it is also observed that the growth rate of CO_2 emissions from the aviation sector is faster in recent decades as compared to road, rail, or shipping sectors. According to the International Energy Agency, after COVID-19 virus restrictions, the CO_2 emissions from the aviation sector in the year 2023 have reached up to 950 Mt CO_2, which is almost 90% of the pre-COVID-19 virus emission level. According to the ICAO, the emissions from the aviation sector could triple in 2050 as compared to 2015. The direct emissions from the aviation sector in 2022 account for 3.8–4% of the total European Union GHG emissions. From the overall transport emissions, the aviation sector generates 13.9% of the emissions, which is the second largest source of the GHG emissions in the transport sector after road transport [4,5]. Sustainable aviation fuels (SAFs), designed to be compatible with existing aircraft and infrastructure, have emerged as a near term solution to decouple aviation growth from environmental degradation.

Parallel to aviation, the road transport sector is also under immense pressure to reduce its carbon footprint. While electrification offers a promising pathway, internal combustion engine (ICE) vehicles are expected to persist, particularly in regions where infrastructure development lags. This scenario underscores the importance of alternative fuels like methanol-derived products, which can serve as drop-in replacements for conventional fossil fuels. Methanol, produced from a variety of feedstocks including natural gas, biomass, and CO_2, offers versatility and potential for significant GHG reductions. Several companies are actively involved in advancing methanol production technologies. Johnson Matthey has been commercializing its technology for converting CO_2 emissions into methanol since 2011. Its well-known process, eMERALD, is recognized as a highly reliable and low-risk approach capable of converting nearly 100% of hydrogen and CO_2. This process significantly minimizes overall energy requirements and operational costs. Johnson Matthey's methanol production technology,

* Corresponding author.
E-mail address: giovanni.manente@unisalento.it (G. Manente).

https://doi.org/10.1016/j.nxener.2026.100543
Received 25 July 2025; Received in revised form 10 September 2025; Accepted 12 February 2026

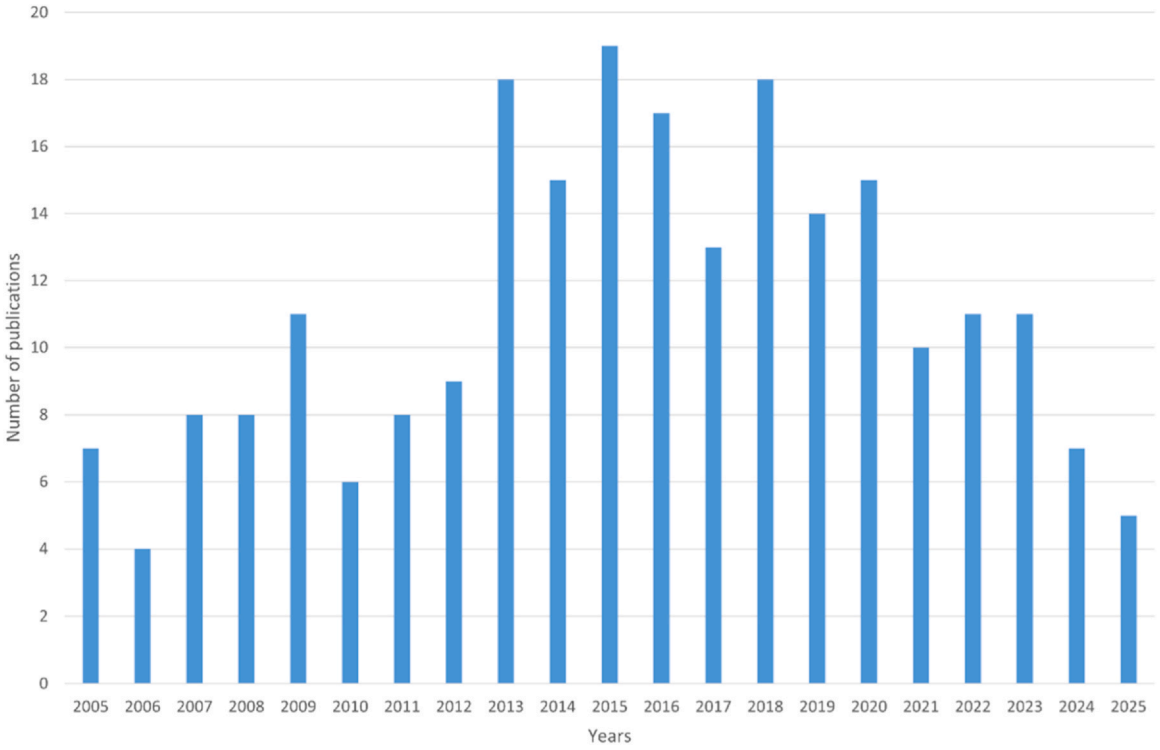

Fig. 1. Number of publications on methanol to gasoline (MTG) in the time span 2005–2025. A declining trend is visible in the last decade.

designed specifically for bio-methanol and e-methanol production, offers a potential global warming reduction of 35–39% compared to the steam methane reforming benchmark, according to the Intergovernmental Panel on Climate Change GWP 100 methodology [6].

Furthermore, the Methanol Institute has partnered with Finland's GENA Solutions Oy to develop a comprehensive database of ongoing and planned projects for e-methanol and bio-methanol production. As of August 2025, this database identified 238 renewable methanol production projects with a total announced capacity of 41.9 million tons (Mt) expected by 2030. Specifically, these projects include an anticipated capacity of 23.4 Mt for e-methanol and 18.5 Mt for bio-methanol. Additionally, the database lists 17 low-carbon (blue) methanol projects, which are projected to deliver an additional capacity of 10.1 Mt by 2030. Considering the barriers and challenges associated with project implementation, the practical capacity of renewable methanol production by 2030 is expected to range between 7 and 14 Mt, accounting for approximately 20–40% of the total pipeline capacity [7]. The Kassø green methanol plant, located in southern Denmark, represents a significant advancement in the production of e-methanol. This facility, considered one of the largest of its kind globally, is designed to produce up to 42,000 tonnes of e-methanol annually. The plant utilizes renewable energy sourced from solar power, harnessing 3 large-scale electrolyzers, each rated at 17.5 MW, to perform water electrolysis. These electrolyzers collectively produce approximately 6000 tonnes of green hydrogen per year, consuming around 90,000 tonnes of water [8]. The generated green hydrogen is then converted into e-methanol through an in-house methanol synthesis process, highlighting the integrated approach to sustainable fuel production adopted by the facility. Additionally, the plant strategically captures and utilizes excess heat generated during the methanol synthesis process, supplying district heating sufficient to serve up to 3300 local households, thereby enhancing the overall energy efficiency and sustainability of the operation. Key industry stakeholders such as Maersk, LEGO, and Novo Nordisk have been identified as primary off-takers of the plant's e-methanol output, demonstrating its applicability across shipping, manufacturing, and pharmaceutical sectors. Concerning the direct use of methanol in thermal engines, it is fairly well known that methanol cannot be used directly as an aviation fuel in jet engines because of its low energy density compared to kerosene, with obvious implications on the flight range. Furthermore, the direct use of methanol would affect the stability and performance of jet engines. According to literature studies, 10% and even 20% of methanol concentration blends with kerosene show a stable engine performance, but 30% of methanol concentration causes substantial speed fluctuations, which results in unstable flight operation [9]. Also, pure methanol cannot be used directly in diesel engines before making some modifications. There are several reasons for not using pure methanol in diesel engines, like its low cetane number, poor ignition characteristics, corrosiveness, and compatibility with the standard diesel injection system [10,11]. We can use methanol as a blend in gasoline engines, but when the concentration exceeds 15%, some modifications are required to avoid corrosion issues. Also, methanol is toxic in nature as compared to gasoline and diesel. Accidental ingestion or prolonged exposure to methanol vapors can lead to serious health issues, including blindness or death [12]. Methanol can be used directly in maritime transport as a fuel. In the year 2023, around 100 methanol-burning ships have been ordered by different key players from the industry, which include Maersk, COSCO Shipping, and CMA CGM [13,14]. Use of methanol in maritime transport can reduce the NO_x emissions up to 90% as compared to the use of conventional fuels. Also, CO_2 emissions can be reduced up to 10% by using methanol. Sulfur-free structure of methanol results in the reduction of SO_x emissions up to 90–97% and 90% reduction in particulate matter emissions [15].

Thus, even though some direct applications of methanol as a transport fuel are possible, its conversion to drop-in fuels fully compatible with the existing infrastructure appears instrumental to extend its applications beyond the shipping sector. In this respect, the methanol-to-gasoline (MTG) and methanol-to-kerosene (MTK) conversion processes represent 2 promising routes for synthesizing transportation fuels tailored to the specific needs of the road and aviation sectors, respectively.

Figs. 1 and 2 show the number of publications on MTG and MTK over the past 20 years. It clearly appears that the scientific interest in

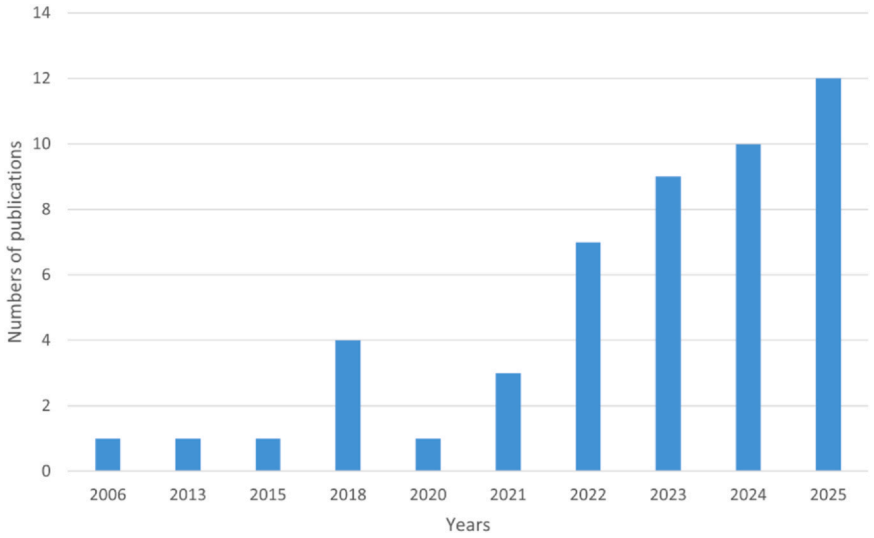

Fig. 2. Number of publications on methanol to kerosene (MTK) in the time span 2005–2025. A rising trend is clearly visible, also considering that the year 2025 has not ended.

MTG first increased and then decreased starting from the mid-2010s because of the achieved technology maturity and market integration. On the other hand, as shown in Fig. 2, the researchers are currently focusing their attention on the emerging MTK technology, due to the global push to decarbonize the aviation sector and the rising demand for SAFs.

Various well-known companies have developed the process for converting methanol into gasoline and kerosene, and they are contributing significantly to global decarbonization strategies in the transportation sector. For the MTG route, ExxonMobil's MTG technology has historically been a pioneering process, commercially demonstrated in the 1980s at the Mobil Synfuels Plant in New Zealand. Today, ExxonMobil licenses this technology globally, with active demonstration plants operating in China and the United States. Another significant contributor, Haldor Topsoe, has developed the TIGAS (Topsoe Improved Gasoline Synthesis) technology, which is implemented at industrial scales, notably in facilities located in China and Turkmenistan, with ongoing international collaborations for further commercialization. Primus Green Energy has also been active in this area through its STG+ (Syngas to Gasoline Plus) technology, closely related to traditional MTG processes, demonstrated through pilot plants in the USA [16–18].

About the MTK technology, Haldor Topsoe's MTJet process exclusively targets the production of SAF from methanol, by using green hydrogen and captured CO_2. Honeywell UOP has developed its methanol-to-jet fuel technology, actively chasing pilot-scale and emerging commercial projects worldwide. Johnson Matthey is also actively working on methanol-to-jet technology, currently in demonstration phases through various collaborative initiatives. Additionally, Vertimass is scaling catalyst-driven technologies that can convert methanol or ethanol into aviation fuels, gasoline, and diesel [6,17,19,20].

The Paris Agreement, signed by 196 countries, aims to limit global warming to below 2 °C above pre-industrial levels, targeting net-zero emissions through substantial transformations in the energy and industrial sectors [21]. This has accelerated research and development in power-to-liquid (PtL) technologies, which utilize renewable electricity to produce synthetic fuels. PtL processes, especially when integrated with direct air capture (DAC) of CO_2, offer the potential for large-scale, carbon-neutral fuel production [22]. In contrast, biomass-to-liquid (BtL) pathways face scalability limitations due to biomass availability [23]. Consequently, comparing MTG and MTK pathways not only addresses the technical and economic aspects of fuel production but also their environmental sustainability and scalability.

This review paper provides a thorough analysis of the MTG and the MTK pathways, focusing on the various aspects of process layouts, equipment, fuel yield, energy efficiency, economics, and suitability for road transport and aviation sectors. The literature survey has allowed the authors to identify some recurrent process schemes, which have been taken in this study as representative of each of the 2 pathways. Within these process configurations, the key sub-systems have been determined/isolated, which characterize the distinctive features of each pathway as well as the differences between MTG and MTK. Accordingly, the comparison between MTG and MTK is directly obtained by the consideration of the presence or absence of these subsystems, and more specifically, of the different modeling strategies employed within each subsystem. The performance metrics of mass yield, chemical energy efficiency, and carbon efficiency have been extracted or calculated from the data of simulation work reported in the literature and shown in uniform plots that directly highlight the differences between the 2 pathways. Moreover, specific design aspects related to the choice of the catalyst, the design of the reactor, and possible challenges have also been summarized in this paper to illustrate specific technological aspects, which can be crucial in the decision process of targeting a specific fuel product or repurposing an MTG plant to MTK. Unlike previous papers focusing on the entire supply chain, this work focuses on the methanol conversion process only, regardless of the source of methanol. This allows a closer look at the methanol conversion process into gasoline or kerosene. The economic paragraph extends the analysis to a wider boundary to show the viability of these renewable fuels, depending on the feedstock for methanol synthesis. At least to the authors' knowledge, there is no such kind of review available in the literature which reports a similar comparison between MTG and MTK, which are often considered as 2 separate subjects due to the different products and target users. Instead, a common base analysis does allow a better understanding of the most recent studies on MTK and the gradual shift of the literature investigations from the MTG to the MTK process.

2. Methanol-to-gasoline pathway: process design, performance, and challenges

The MTG pathway provides an alternative to other gasoline production processes by converting methanol derived from various feedstocks, such as biomass, coal, and natural gas, as well as hydrogen and CO_2 (Fig. 3). This section presents an overview of the MTG process, discussing key aspects including the process design, catalysts employed,

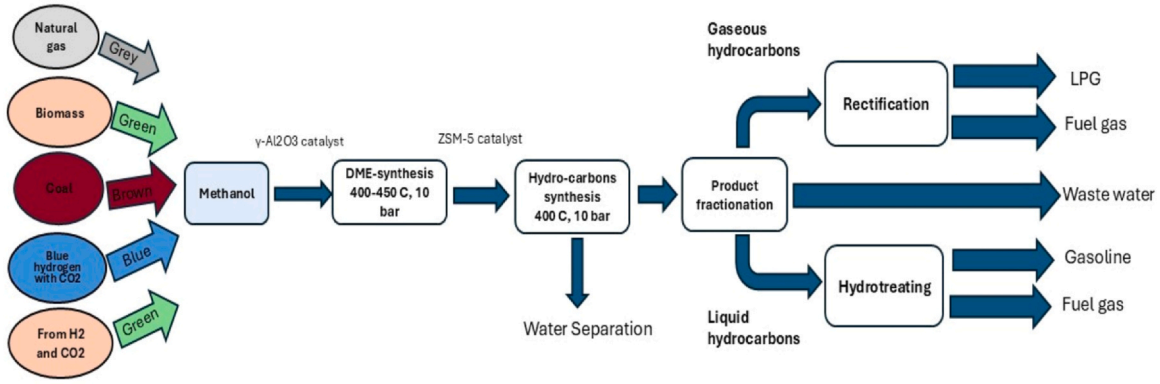

Fig. 3. Schematic flowchart for the methanol to gasoline pathway.

reactor configurations, and associated performance indicators. Additionally, it addresses major challenges and evaluates crucial factors impacting the practical and economic viability of this alternative gasoline production method.

2.1. MTG process overview

Gasoline is an important hydrocarbon-based fuel widely used in ICEs as well as in the petrochemical industries. Conventionally, it is produced through the fractional distillation of crude oil, and it is primarily composed of light to medium alkanes, with aromatics serving as octane enhancers. However, because of the environmental effects and concerns related to global warming, the use of aromatic compounds has been reduced [24–28]. In addition, natural crude oil reservoirs are depleting, and the demand for energy is growing rapidly, which is why the need for sustainable energy solutions is vital. The MTG process has emerged as a viable alternative to produce high-quality gasoline [29–31].

The basic course in the MTG process is the conversion of methanol into olefinic and aromatic hydrocarbons with the help of ZSM-5 zeolite catalyst. A simplified block diagram for such conversion is shown in Fig. 3, where 2 primary steps can be noticed. In the first step, methanol is dehydrated into dimethyl ether (DME) over mildly acidic oxides like γ-Al_2O_3 [32]. In the second stage, the zeolite catalyst (e.g., ZSM-5) facilitates the conversion of DME and methanol into gasoline-range hydrocarbons by methylation, cracking, and aromatization of olefins [33,34]. These reactions produce hydrocarbons with high octane ratings (90–100), achieving 80% selectivity for gasoline, with Liquefied Petroleum Gas (LPG) as the primary by-product [35]. The network structure of ZSM-5, including its microporous channels, promotes shape-selective catalysis, which is essential for producing high-quality gasoline [36]. A simple mechanism of the reactions involved in this process is given below [37]

$$CH_3OH \leftrightarrow \quad CH_3OCH_3 \quad + \quad H_2O \tag{1}$$

$$CH_3OCH_3 \quad \rightarrow \text{light olefins} + \quad H_2O \tag{2}$$

$$\text{Light olefins} \rightarrow \text{higher olefins} + \text{paraffins} + \text{aromatics} + \text{napthenes} \tag{3}$$

Industrial implementation of the MTG process began in the 1980's with Mobil's commercial plant in New Zealand. With the production capacity of 14,500 barrels per day (bpd), this facility used syngas-derived methanol as feedstock. It employed a fixed-bed reactor configuration, producing clean gasoline with properties comparable to conventional fuels [38–40]. Although this plant ceased MTG operations in the 1990's due to low fossil fuel costs, advancements in MTG technology have renewed interest in this process again. For example, ExxonMobil and Uhde Corporation have developed coal-to-gasoline processes in the United States and China, with capacities of up to 22,000 bpd. These modern facilities incorporate carbon capture technologies to mitigate CO_2 emissions [41,42]. TOPSOE's TIGAS process further optimized MTG operations, achieving improved scalability and efficiency [43].

The reaction mechanism of the MTG process involves complex pathways, which include a hydrocarbon pool mechanism, in which adsorbed methylbenzenes act as auto-catalysts to promote alkylation with methanol and DME. Chain growth and successive cracking steps produce paraffins, olefins, and aromatics. Regardless of its commercial success, the MTG process faces challenges such as catalyst deactivation because of the coke deposition, which requires regular regeneration cycles for the catalyst. Multiple kinds of research are still ongoing, where the focus is on optimizing catalyst pretreatment methods and reaction conditions to improve catalyst lifetime and efficiency [36].

2.2. The choice of catalyst in gasoline synthesis

Catalysts play a vital role in the methanol/DME to gasoline conversion, affecting the efficiency, yield, selectivity, and economic feasibility of the overall process. Among the various types of catalysts, ZSM-5 zeolite is considered to be the most effective due to its unique structural and chemical properties. Its shape-selective microporous structure with 10-ring channels enables the selective formation of gasoline-range hydrocarbons while minimizing the formation of less desirable products [44].

With the help of metal doping and structural adjustment of the ZSM-5 catalyst, its performance can be further enhanced. For example, the loading of copper oxide (CuO) and zinc oxide (ZnO) onto ZSM-5 catalysts has improved selectivity and reduced coke formation during the MTG process. CuO/HZSM-5 improves hydrogen transfer reactions [45], leading to a higher yield of paraffinic hydrocarbons, while ZnO/HZSM-5 promotes olefin stability and reduces coke deposition by facilitating effective cyclization reactions. Additionally, optimizing the Si/Al ratio in the ZSM-5 catalyst affects its acidity [46]. With a higher Si/Al ratio, the life of the catalyst and the aromatic content of the gasoline also increase, thus improving its octane number.

Coke formation, which is one of the major challenges in the MTG process [47], is effectively controlled and decreased by adjusting the acidity and structural properties of the catalyst (see e.g. [48,49]). Post-synthesis modifications such as desilication or surface impregnation with metals can further increase the resistance of the catalyst to coking [50].

Other than an increase in yield and coke reduction, ZSM-5 and its modified versions provide other benefits, such as high thermal stability, which allows the reduction of the regeneration frequency of the catalyst [51]. With the help of this stability of the catalyst, the cost can be reduced, and the efficiency of the process can be increased.

Some examples of different catalysts, their operating conditions, and features are given in Table 1.

Table 1
Catalyst types, parameters, and performance indicators for the e-gasoline synthesis in the MTG process

Catalyst	Operating conditions	Product yields and key features	Comments	Refs.
HZSM-5	Temperature: 350–400 °C, Pressure: 1–2 MPa, WHSV: 1–2 h^{-1}	Gasoline: 80%, LPG and light gases: 20%	High selectivity for C_5–C_{12} hydrocarbons. Prominent shape-selectivity due to microporous structure	[52]
CuO/HZSM-5	Temperature: 390–420 °C, Pressure: 2 MPa, WHSV: 1.5–2.5h^{-1}	Gasoline: 85%, Reduced durene formation	Promotes hydrogen transfer reactions. Enhances aromatic stability and reduces coke formation	[53]
ZnO/HZSM-5	Temperature: 380–400 °C, Pressure: 1 MPa, WHSV: 1.8h^{-1}	Gasoline: 78%, Increased aromatics selectivity	Facilitates cyclization and aromatization reactions. Improves thermal stability of catalyst	[54]
Modified ZSM-5 (high Si/Al ratio)	Temperature: 350 °C, Pressure: 1 MPa, WHSV: 3h^{-1}	Gasoline: higher selectivity, reduced coke formation	Higher Si/Al ratio decreases total acidity, promoting longer catalyst life and enhanced selectivity to olefins and aromatics	[48]
Zn/MCM-41	Temperature: 450 °C, Pressure: 0.5 MPa, WHSV: 10h^{-1}	Gasoline: 70%, Increased paraffins	Large mesopores improve mass transfer. Higher paraffin content due to efficient hydrogen transfer reactions	[55]
HZSM-5 with Al-P modification	Temperature: 420 °C, Pressure: 1 MPa, WHSV: 3.5h^{-1}	Gasoline: 83%, Reduced light olefins	Enhanced catalyst lifetime. Phosphorus improves structural stability under reaction conditions	[48]
Cu-Zn-Al/HZSM-5	Temperature: 400–450 °C, Pressure: 2 MPa, WHSV: 2h^{-1}	Gasoline: 88%, increased aromatic content	Combination of metal oxides improves conversion efficiency and aromatic yield	[35]
Hollow-capsule ZSM-5	Temperature: 390 °C, Pressure: 1 MPa, WHSV: 3.18h^{-1}	Gasoline: 90%, reduced coke formation	Mesoporous shell structure facilitates better diffusion and reduced coking. Longer catalyst lifetime	[56]

LPG = Liquefied Petroleum Gas; MTG = methanol-to-gasoline; WHSV = weight hourly space velocity.

2.3. The reactor design in MTG

The MTG process uses different types of reactors to enhance conversion efficiency, product selectivity, and operational stability. At the beginning, fixed bed reactors were used (e.g., in the Mobil MTG process), composed of a dual reactor system to separate the 2 steps of dehydration of methanol and synthesis of hydrocarbons. In the first reactor, methanol was dehydrated to DME in the presence of γ-Al_2O_3 catalyst, then in the second reactor, the produced DME was converted into gasoline hydrocarbons in the presence of ZSM-5 catalyst. These reactors for the production of DME and gasoline hydrocarbons usually operate at pressures around 33 bar and temperatures around 380 °C, providing a controlled environment for high conversion rates while managing the coke formation [52,57].

Fluidized-bed reactors provide a more advanced approach for methanol conversion, featuring continuous catalyst regeneration during the process to maintain long-term operational stability. In the case of fluidized bed reactors, both the methanol dehydration and hydrocarbon synthesis are performed in a single unit. The operating conditions for such reactors are 400 °C of temperature and approximately 14 bar of pressure. The main features of such kind of reactors are their effective heat management and controlling the coke deposition, which are the critical factors that can affect the catalyst life and also can enhance the yield [58,59]. A specific configuration, the 2-zone fluidized bed reactor, combines the reaction and regeneration zones within a single reactor, allowing for continuous operation and further reducing downtime. This design is particularly effective in controlling the exothermicity of the MTG reactions [55].

Pilot-scale studies often explore tradeoffs between process efficiency, coke formation, and product distribution using both fixed-bed and fluidized-bed reactors. Improvements, such as the use of multiple reactors in series with interstage cooling, have been proposed to handle the significant heat release during exothermic MTG reactions. These approaches aim to maximize gasoline yield while maintaining operational efficiency [58]. Furthermore, the suitability of repurposed catalytic reforming units in the MTG process was investigated. Optimized reactor lengths and customized catalytic formulations have been shown to improve product yields under simulated conditions significantly [57].

Key reactor specifications in the MTG process include the use of ZSM-5 zeolite catalysts, known for their shape-selective properties that limit hydrocarbon chain growth to the gasoline range. Temperature control is critical due to the highly exothermic nature of the reactions, as excessive heat can lead to rapid deactivation of the catalyst. Operating pressures generally range between 13 and 50 bar, ensuring high reaction rates and effective product separation. Gas space velocity values vary widely, from 1000 h^{-1} to 10,000 h^{-1}, depending on the reactor configuration and specific design objectives [58].

Different reactor types used in the MTG process, their advantages and disadvantages, and their operating conditions are shown in Table 2.

2.4. Design of methanol-to-gasoline plants

MTG plants are composed of a sequence of processes basically consisting of dehydration of methanol, synthesis of different hydrocarbons, and separation of the desired products. Even though the MTG plant layouts reported by different authors may slightly differ, some recurrent schemes have been identified, which are summarized below.

In the study by Arias Gallego et al. [57], methanol is sourced from various origins, including gray methanol derived from natural gas and green methanol produced through CO_2 hydrogenation. The plant configuration combines the ExxonMobil layout with some process units defined by Rojas [60,61]. First, the methanol enters the catalytic fixed bed reactor filled with γ-Al_2O_3 catalyst, where the dehydration of methanol (Eq. 1) takes place under controlled conditions of 440 °C and 10 bar to achieve a methanol conversion to DME equal to 90%. The

Table 2
Different reactors, configurations, and operating conditions used in the MTG process

Reactor type	Configuration	Operating Conditions	Advantages	Disadvantages	Refs.
Fixed-bed reactor	Dual-reactor system (methanol dehydration and hydrocarbon synthesis)	Pressure: ~33 bar, Temperature: 380 °C	Simple design, high gasoline yield	Catalyst deactivation due to coke formation requires periodic regeneration	[52,57]
Fluidized-bed reactor	Single unit with continuous catalyst regeneration	Pressure: ~14 bar, Temperature: 400 °C	Continuous operation, effective heat management, and reduced downtime	Higher operational complexity	[58,59]
Two-zone fluidized bed reactor (TZFBR)	Reaction and regeneration zones combined in 1 unit	Pressure: 14–30 bar, Temperature: 400–450 °C	Continuous operation, efficient coke removal, heat control	Complex reactor design	[55,58]
Multistage reactor system	Multiple reactors in series with interstage cooling	Pressure: ~30 bar, Temperature: 400–450 °C	High gasoline yield, improved temperature control	Higher capital costs, increased operational complexity	[58]
Repurposed catalytic reforming unit	Modified for MTG processes	Pressure: 30–50 bar, Temperature: 400–450 °C	Utilizes existing infrastructure, lower capital investment	May require catalyst and configuration optimization	[57]

MTG = methanol-to-gasoline.

product from the DME production reactor is sent to a set of parallel packed bed catalytic reactors (operating at 400 °C and 10 bar), where the hydrocarbon synthesis takes place in the presence of ZSM-5 catalyst. The reactor effluent is cooled with heat recovery, and the separated gases are recycled to the e-gasoline reactor. [62]

The raw gasoline, composed of higher olefins, paraffins, and aromatics, after water removal, undergoes refining by passing through 3 distillation columns, which include: i) a de-ethanizer; ii) a stabilizer for removing the light gases like LPG; iii) a gasoline splitter to isolate the heavy aromatic compounds such as durene from gasoline. The durene-rich hydrocarbons are sent to a hydro-isomerization reactor (modeled using an R-Stoich reactor in Aspen Plus) operating at 345 °C and 16 bar. The resulting light gasoline from the splitter and the treated heavy gasoline are mixed together to produce high-quality gasoline with the desired octane numbers, low sulfur content, and aromatic content in the range 25–35%.

Besides Arias Gallego et al. [57] other authors, like E-Moghaddam et al., Galadima et al., Gonzalez et al., and Liu et al. [38,39,62,63] considered basically the same layout as shown in Fig. 4, which is essentially based on the ExxonMobil plant for the production of gasoline from methanol.

In the plant layout considered by Hennig and Haase et al. [59], which has been redrawn in Fig. 5, the MTG process was part of a hydrogen-enhanced BtL plant, where the conversion of biomass-derived syngas into methanol was followed by its conversion into gasoline.

First, the produced methanol was preheated and sent to the DME reactor, which was modeled using the R-Equil model in Aspen Plus, assuming chemical equilibrium at 250 °C. The produced mixture of DME and unconverted methanol was again heated and sent to the gasoline synthesis reactor. The hydrocarbon synthesis reaction took place at 380 °C and 33 bar, producing a mixture of different hydrocarbons with a significant percentage of gasoline fraction [65]. The distribution of the product mainly depends on reaction conditions and the catalyst design, having 70% of aromatics in the gasoline composition. The effluent from the e-gasoline reactor was cooled with heat recovery and sent to a flash separator, where light hydrocarbons were separated from the raw gasoline mixture. After water separation, the gasoline fraction was sent to a hydrotreating reactor, which operated at mild conditions, 240 °C and 34 bar, reducing the aromatic content in gasoline to below 35% by volume [66]. After hydrotreating, the hydrogen gas was recycled, and gasoline was obtained as the bottoms of a final distillation column. Note that, unlike the previous plant configuration, the light gases are not recycled to the e-gasoline reactor but are directly sent to a column for LPG product recovery. Moreover, in this layout, all the gasoline fraction passes through the hydrotreating reactor.

2.5. *Different modeling approaches of MTG*

All the MTG flowsheets considered shared the same subsections, namely DME synthesis, hydrocarbons production in the gasoline range, water separation, gasoline refining, and hydrotreating. Most of the studies, like E-Moghaddam et al. [62], Galadima et al. [38], Gonzalez et al. [39] are based on the ExxonMobil layout and related experimental findings, while the study by Hening and Hasse et al. [59] is based on the experimental study done by Chang and Silvestri et al. [64]. The identified differences in flowsheet layout and modeling strategy between Arias et al. [57] and Hennig et al. [59] are taken here as representative of 2 separate modeling approaches of the MTG process, which are recurrent in the literature.

- *DME production*: Regarding the DME synthesis, an R-Stoic reactor is included in the first flowsheet (Arias et al. [57]) for the modeling of the production of DME/light olefins using a γ-Al_2O_3 catalyst. The reactor data are based on the ExxonMobil plant [60]. In contrast, Hennig et al. [59] use an R-Equil reactor for DME/light olefin

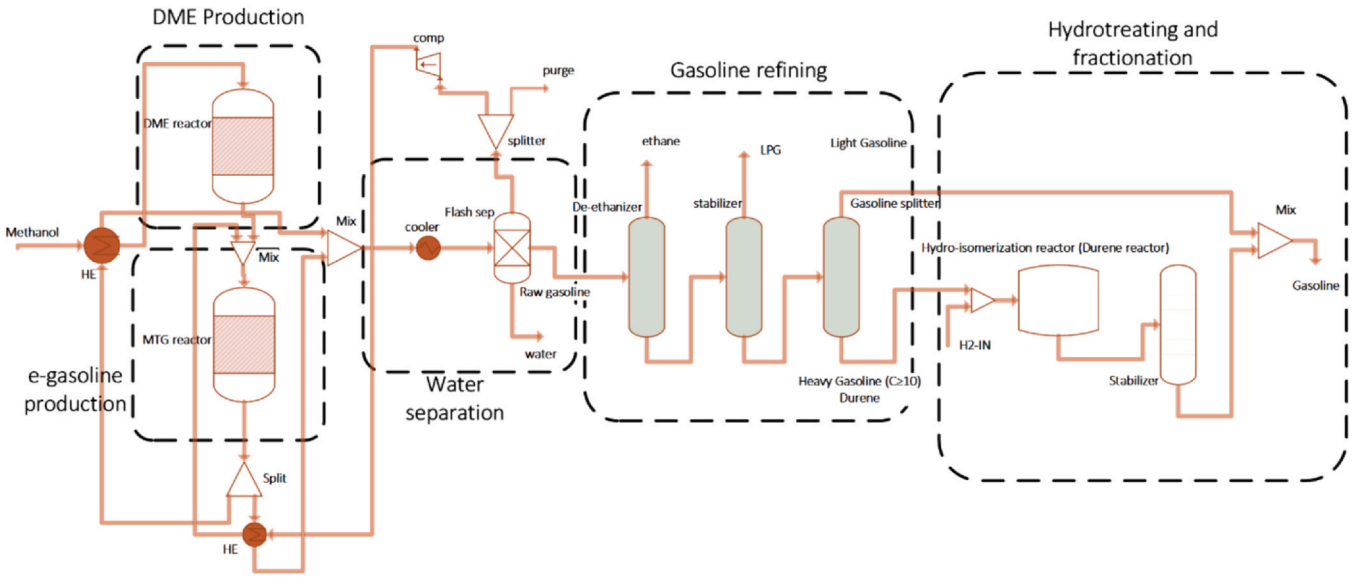

Fig. 4. Process flow diagram of MTG plant based on the ExxonMobil process, considered in Arias Gallego et al. [57] as well as by other authors [38,39,63,64]. DME = dimethyl ether; MTG = methanol-to-gasoline.

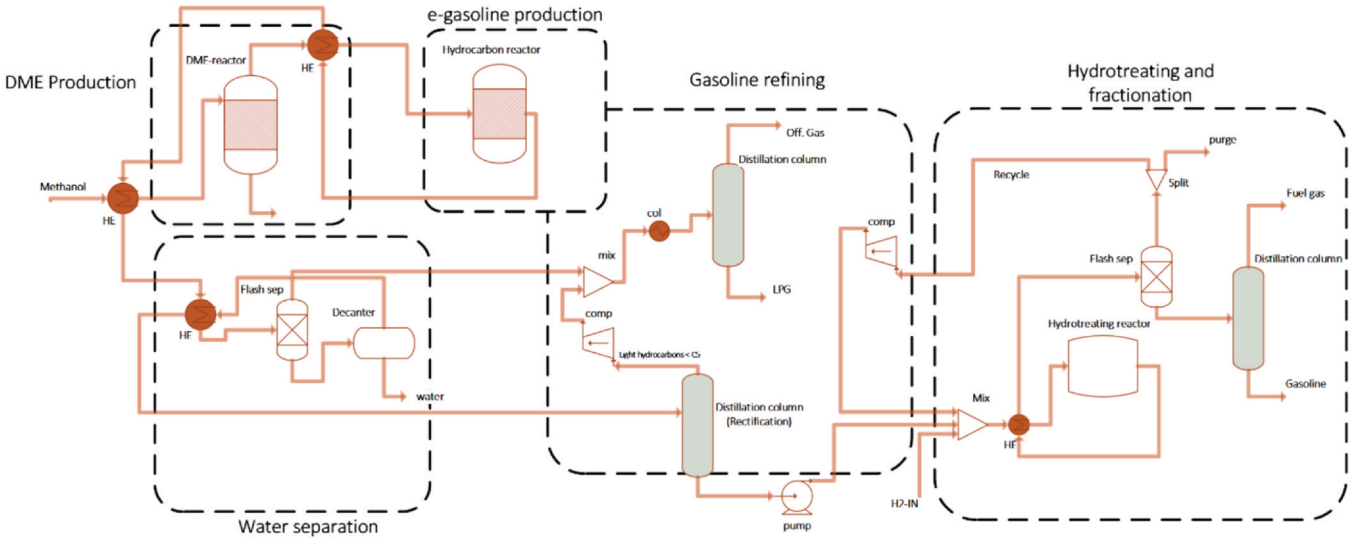

Fig. 5. Process flow diagram of MTG plant based on the study of Hennig and Haase et al. [59]. DME = dimethyl ether; MTG = methanol-to-gasoline.

production, relying on the minimization of Gibbs free energy to determine chemical equilibrium composition [65].

- *E-gasoline production*: The modeling of the e-gasoline/hydrocarbons synthesis section was either based on a kinetic model [57] or a yield reactor. In the first flowsheet, 3 packed-bed kinetic reactors (R-Plug) operated in parallel, utilizing a lumped kinetic model developed from the experimental work of Choe et al. [66]. In the second flowsheet, an R-Yield reactor was implemented based on the experimental data from Chang and Silvestri [64,67].
- *E-Gasoline refining*: The e-gasoline refining section also exhibits some differences. The first flowsheet [57] uses 3 distillation columns in series to refine the produced gasoline. The first column removes ethane and other light gases, the second one serves as a stabilizer to separate LPG, whereas the third column is a gasoline splitter, whose function is to separate heavier aromatics ($\geq C_{10}$), particularly durene, which is prone to solidification due to its high melting point (T_m = 79 °C) [68]. The separated durene is then sent to the hydrogenation section. Conversely, in the second flowsheet (Hennig et al. [59]), only 2 distillation columns are used. The first, known as the degassing column, separates the light hydrocarbons ($< C_5$) dissolved in the organic liquid phase from the bottoms. All the bottom product is sent to the hydrotreating section for further processing. The second column is used to separate the off-gas from the LPG.
- *Hydrogenation*: The hydrogenation section in both processes is nearly identical. In the first flowsheet [57], durene undergoes hydro-isomerization in a reactor containing sulfided base metal catalysts, to produce 2 durene isomers with significantly lower melting points: isodurene (T_m = −24 °C) and prehnitene (T_m = −7 °C) [69]. The hydrogenation reaction is modeled using an R-Stoic reactor with given durene conversion [70]. The light gasoline fraction from the gasoline splitter is finally blended with the hydrotreated durene to obtain the gasoline product. Meanwhile, in the second flowsheet [59], the raw gasoline from the bottoms of the degassing column is sent to a hydrogenation reactor to reduce the aromatics content to the 35% target and to transform olefins to their fully hydrogenated species. Here, the hydrogenation reaction is modeled according to the findings by Wilson et al. [71] about the hydrogenation of mixed aromatics at mild conditions.

Table 3
Main fuel product and co-products considered in the different studies on MTG

Primary purpose of the plant	Other useful fuel products	Note	Refs.
Production of gasoline	No	Recycle of unconverted gases into e-gasoline reactor	Arias Gallego et al. [57]
	LPG	High selectivity in gasoline	E-Moghaddam et al. [62]
	LPG	Low selectivity in gasoline	Hennig and Hasse et al. [59]
	LPG	Investigation of the process parameters to maximize gasoline yield	NREL report [58]

LPG = Liquefied Petroleum Gas; MTG = methanol-to-gasoline; NREL = National Renewable Energy Laboratory.

2.6. Performance of the methanol to gasoline pathway

In this section, the performance metrics reported in the literature for the MTG pathway are shown in different plots focusing on mass yields, chemical energy efficiency, and carbon efficiency. Besides the 2 representative studies of MTG described above, 2 additional studies have been added to obtain a more complete picture of the potential of the MTG pathway. Table 3 summarizes the primary purposes of the examined plants and the main co-products.

2.6.1. Mass yield

Studies such as the National Renewable Energy Laboratory (NREL) report [58] show that the highest yields of gasoline are achieved under optimized conditions of temperatures (350–400 °C), pressures (15–25 bar), and by using the ZSM-5 catalysts. The effects of process parameters like gas hourly space velocity and water content in the methanol feed also play a critical role in maximizing the gasoline yield [39,58].

Fig. 6 shows the MTG mass yields and methanol to all liquid fuel products (i.e., gasoline plus LPG) mass yields under optimized conditions. It can be seen that the mass yield of gasoline in most of the studies is in the range 35–36 wt%. A lower value of only 21.4 wt% is reported in Hennig and Hasse et al. [59], due to the absence of recycle of light gases.

The percentage of the gasoline product with respect to all liquid fuel products (i.e., gasoline and LPG) is shown in Fig. 7. While in Arias Gallego et al. [57] the only useful product considered is e-gasoline, some variable fractions of LPG are co-produced in the other plants. In the NREL report [58], the mass yield of gasoline achieves a remarkable value of almost 90 wt% because of the high selectivity of the catalyst towards gasoline range hydrocarbons. Instead, the gasoline fraction is less than 60% in Hennig and Hasse et al. [59].

2.6.2. Chemical energy efficiency

The MTG process has demonstrated the ability to achieve chemical energy efficiencies exceeding 85% when integrated with heat recovery systems. Indeed, the high exothermicity of the dehydration and hydrocarbon synthesis reactions allows for effective energy utilization, reducing the external heat requirements for the downstream process units. Industrial applications, such as the Mobil New Zealand facility, demonstrated the potential for heat integration to offset operational costs and improve sustainability [52,58].

The chemical energy efficiencies of MTG and methanol to all liquid fuel products are shown in Fig. 8. The MTG chemical energy efficiency is found mostly in the range 70–73%, with the exception of Hennig and Hasse et al. [59] that report a value of approx. 50% due to the above mentioned reasons. When considering both gasoline and LPG as fuel products, the chemical energy efficiency increases by up to 15% points, reaching maximum values around 88%.

2.6.3. Carbon efficiency

Carbon efficiency shows the amount of carbon that was initially present in the methanol feed finally retained in the gasoline product (and possibly in the LPG co-product), as shown in Fig. 9. The carbon efficiency values for MTG are mostly in the range 78–81%, which are also aligned with the chemical energy efficiency figures. When the sum of gasoline plus LPG is considered, the carbon efficiency is maximum (97%) in the study of E-Moghaddam et al. [62], yet it reaches values exceeding 90% also in the NREL study. As already noticed for the other metrics, there is a significant gap between the carbon efficiency of gasoline production and all fuel products (gasoline plus LPG) in Hennig and Hasse et al. [59] due to the high LPG production. Carbon losses mainly occur through off-gases (e.g., CO_2, light hydrocarbons). However, coke formation on the surface of the catalyst used in the hydrocarbon synthesis reactor and its burning off by air during catalyst

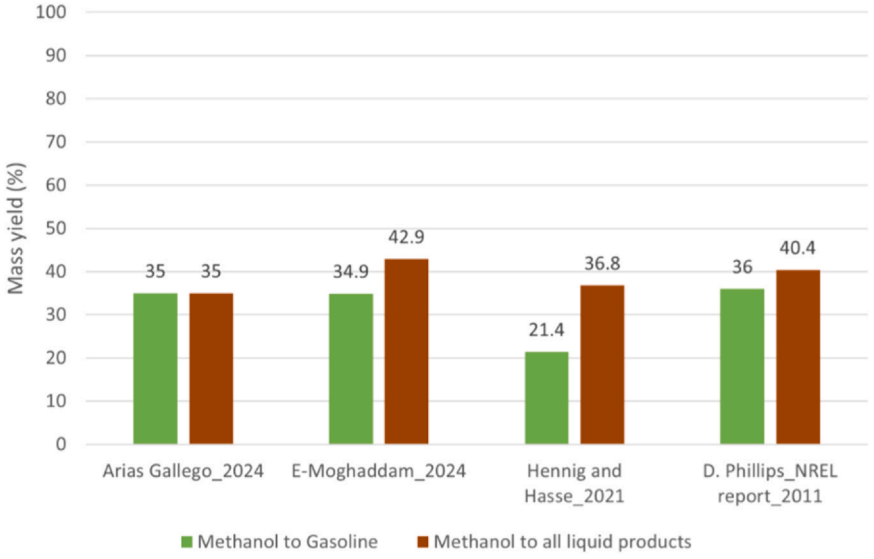

Fig. 6. Mass yields of methanol to gasoline and methanol to all liquid fuel products (gasoline plus LPG) in the MTG process taken from selected studies. MTG = methanol-to-gasoline; LPG = Liquefied Petroleum Gas.

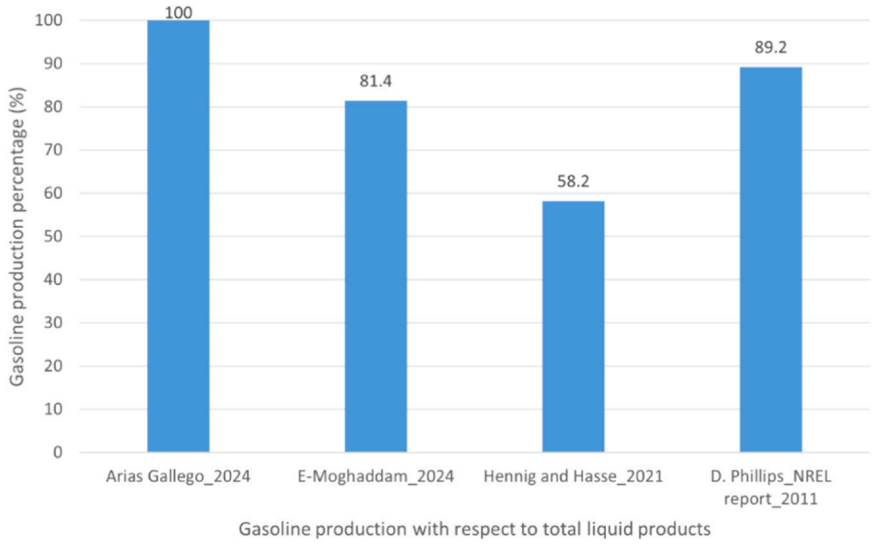

Fig. 7. Share of gasoline compared to total liquid fuel products (gasoline plus LPG). Note that Arias Gallego et al. (2024) considered gasoline as the only useful product. LPG = Liquefied Petroleum Gas.

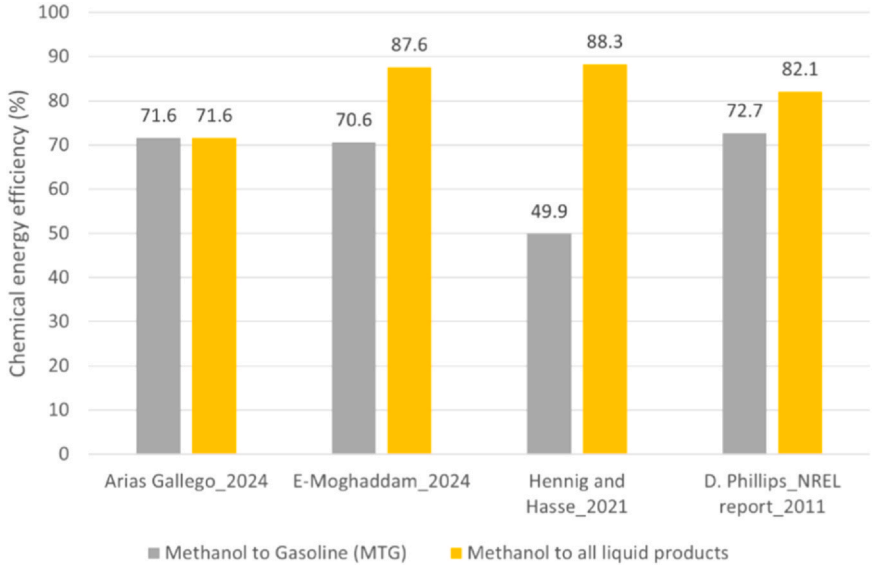

Fig. 8. Chemical energy efficiency of methanol to gasoline and methanol to all liquid fuel products (HHV-based). HHV = Higher Heating Value.

regeneration may also contribute to these losses. Yet, all the studies considered neglect coke in terms of product distribution on the rationale that its yield is typically lower than 0.2% of the methanol feed [59].

2.7. Challenges of the MTG pathway

The MTG process, while offering an alternative pathway for producing high-quality gasoline from methanol, encounters several operational and catalytic challenges. These issues primarily revolve around catalyst deactivation, process efficiency, and economic feasibility.

- *Catalyst Deactivation*: One of the major problems in the MTG process is the deactivation of catalysts, specifically the ZSM-5 catalyst, and it occurs because of the coke deposition. Coke is formed during the hydrocarbon synthesis reaction, and when the produced polyaromatic hydrocarbons are condensed, the coke also condenses on the surface of the catalyst, which causes the blockage of catalyst pores and covers the active sites of the catalyst, and hence, the performance of the catalyst reduces and requires regular regeneration cycles [56]. Moreover, if the reactor is operating at high temperature, then there is a chance of formation of hard coke, which is more difficult to remove; on the other hand, if the reactor is operating at too low temperatures, then deposition of volatile species can occur on the active sites of the catalyst, which again leads to the catalyst deactivation [56]. Besides this, the stability of ZSM-5 catalyst can also be affected by steam during the regeneration process, which can cause irretrievable structural damage to the catalyst and hence affect the durability of the catalyst and also the economic feasibility of the process [72].
- *Reaction Optimization*: Catalyst performance and product distribution can also be affected significantly by the operating conditions, such as reactor temperature, pressure, and weight hourly space velocity. Nonideal conditions can lead to increased coke formation, low methanol conversion, and undesirable product selectivity, such as excessive durene formation, which affects the quality of gasoline. Hence, attaining the balance between higher methanol conversion, optimal gasoline yields, and minimum catalyst deactivation remains a permanent challenge [56].

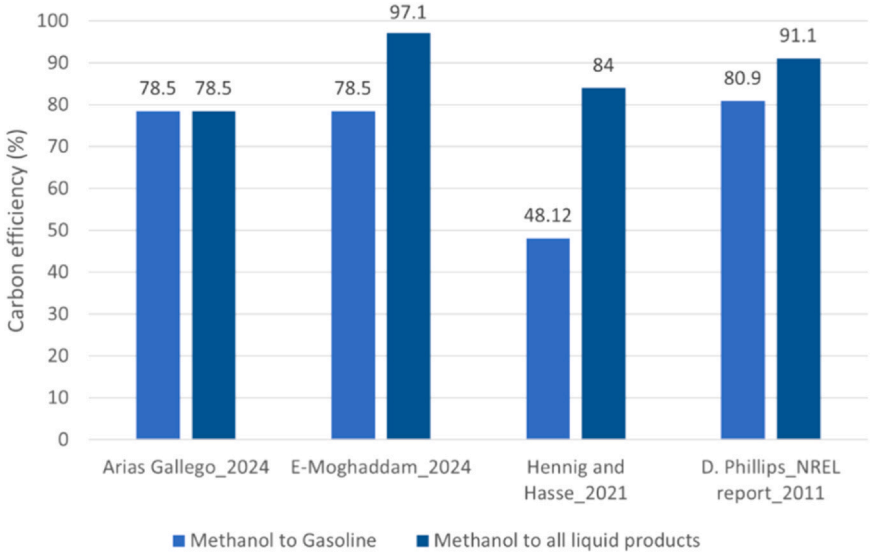

Fig. 9. Carbon efficiencies of MTG processes reported by different authors. MTG = methanol-to-gasoline.

- *Process Scale-Up and Economic Constraints*: Moving from a pilot-scale to a commercial-scale MTG plant involves different design and economic challenges. For example, maintaining stable reaction conditions on large catalytic beds requires accurate temperature control and efficient heat management to avoid hot spots that can intensify the coke formation [58,72]. Moreover, the huge capital and operating costs of large-scale MTG plants, along with the need for robust catalyst regeneration systems, limit the extensive adoption of this technology [57,58].
- *Environmental and Product Quality Concerns*: The formation of coke during the MTG process not only deactivates the catalyst but also contributes to GHG emissions during the regeneration process. Additionally, the composition of gasoline produced from the MTG process, which includes higher concentrations of aromatic compounds than conventional gasoline, raises concerns about the performance of the ICEs and their emission profiles [58,73].
- *Mitigation Strategies*: To address and cover these kinds of challenges, the development of ordered and mesoporous ZSM-5 catalysts, having high resistance to the deposition of coke and having a long active life [74]. Improvements in process optimization, such as the integration of kinetic modeling and advanced heat management systems, are also needed to improve the efficiency of the process and reduce the cost [57]. In this regard, a novel integrated configuration was proposed in Palizdar [75] to improve the MTG process profitability. The MTG plant was the last section of the process value chain and was designed to require the minimum amount of energy from external sources. Besides high octane gasoline, the polygeneration plant produced a variety of products, including liquefied natural gas, liquid helium, and liquid CO2, which improved the economics compared to a standalone MTG plant. The integration of Organic Rankine Cycles in MTG plants to recover the thermal energy from reactors' effluents has been investigated in Liu et al. [76]. The production of electricity at 18.3% thermal efficiency and the reduction of the cooling water demand were found to be valuable for industrial applications.

3. Methanol-to-kerosene pathway: process design, performance, and challenges

The MTK pathway presents a promising alternative to conventional kerosene production methods by converting methanol derived from feedstocks such as biomass, coal, and natural gas into SAF. This section provides a detailed overview of the MTK process, including key stages such as methanol-to-olefins (MTO), oligomerization, and hydro-processing, shown schematically in Fig. 10. It discusses various catalysts employed across these steps, as well as reactor configurations used to optimize the process. Additionally, critical process challenges, including catalyst deactivation, reactor stability, and economic considerations, are addressed. Finally, the performance analysis of the MTK process, covering essential metrics such as mass yield, energy efficiency, and carbon efficiency, is examined to highlight its viability and areas requiring further development.

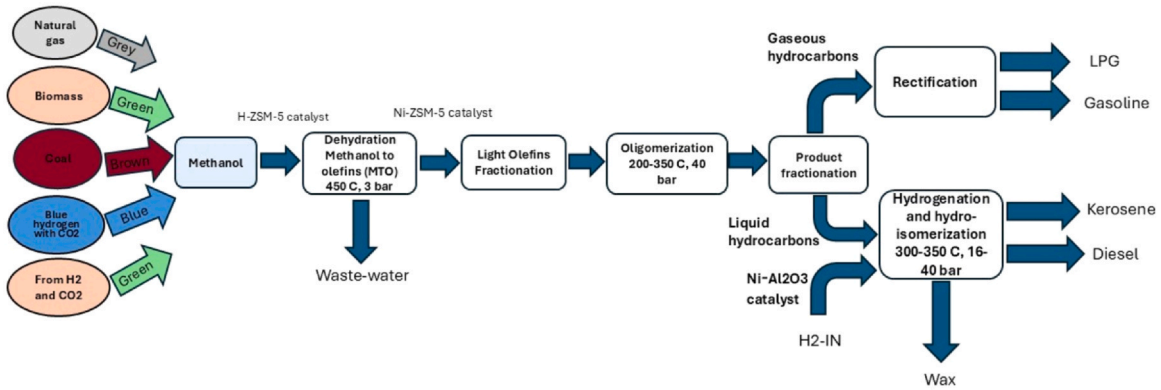

Fig. 10. Schematic flowchart for the methanol to kerosene (MTK) pathway.

3.1. MTK process overview

From an aviation perspective, converting methanol into liquid hydrocarbons is an attractive option for producing synthetic jet fuel. In addition to the established MTG process, Mobil's Methanol-to-Distillate process has demonstrated methanol's conversion into middle distillates, including kerosene and diesel. Both processes rely on shape-selective zeolite catalysts, particularly ZSM-5 [77,78]. The methanol-to-distillates process involves methanol's dehydration and subsequent conversion into light olefins. These olefins undergo oligomerization into higher hydrocarbons, followed by mild hydrotreatment to produce branched (iso-) paraffins, cyclic paraffins, and aromatic compounds. The process can be optimized to yield more than 80% of the desired product fraction (distillate or gasoline) [78]. The reaction system for the synthesis of kerosene is described in the form of general equations below [79,80]. In Eqs. (4) and (5), proposed by Dahl and Kolboe [81], methanol is first dehydrated into DME, and then DME is converted into light olefins, which is shown by a general expression $(CH_2)_n$, where $2 \leq n \leq 4$. The main reaction products from Eq. 5 are light olefins; there are also some light paraffins, naphthenes, and aromatics having carbon number ≤ 10 formed in this reaction [82]. In the final third Eq. (6), light olefins are converted into higher olefins in the range of C_5-C_{20} with the help of an oligomerization process.

$$2nCH_3OH \leftrightarrow \quad nCH_3OCH_3 \quad + \quad nH_2O \tag{4}$$

$$nCH_3OCH_3 \quad \rightarrow 2(CH_2)_n + \quad nH_2O \tag{5}$$

$$2(CH_2)_n \quad \rightarrow \quad C_{2n}H_{4n} \tag{6}$$

Mobil's methanol-to-distillates process was demonstrated as early as the 1980s, achieving favorable yields, efficiencies, and selectivity [77,78]. The distillate fractions meet essential diesel and jet fuel specifications, including the minimum 8% aromatic content required by ASTM D7566 for synthetic jet fuels. Despite these positive features, the MTK process has not yet been commercialized, nor has it undergone ASTM approval. The problem of this issue appears related to the low TRL of the overall MTK pathway as well as the low content of aromatics [83]. Comprehensive analyses are necessary to validate its suitability as a drop-in fuel [77]. This process highlights the potential of methanol as a sustainable platform for producing kerosene-range fuels. However, its commercial implementation requires overcoming challenges related to certification and optimization for large-scale deployment.

3.2. The choice of catalysts in MTK processes

There is a series of catalytic steps occurring in the MTK pathway, which allow methanol to be converted into hydrocarbons in the kerosene range. All the stages present in this process, namely i) MTOs, ii) the oligomerization stage, and iii) the hydro-processing stage, highly rely upon the choice of the catalyst to achieve high efficiency, good selectivity, and higher yield.

i) The first stage, which is MTOs, is commonly carried out in the presence of zeolite-based catalysts; among them, HZSM-5 is widely used. Its strong acidity and thermal stability, combined with its shape-selective properties, enable it for the efficient conversion of methanol into light olefins such as ethylene and propylene. The reaction mechanism involves the formation of DME as an intermediate product, followed by further reactions to produce light olefins. By adjusting the acidity and pore structure of HZSM-5 catalyst, it allows the optimization of olefin selectivity, making it the preferred catalyst for this step [67,84].
ii) In the second step, which is the oligomerization stage, light olefins are transformed into higher hydrocarbons suitable for kerosene production. For this stage, nickel-based catalysts, such as Ni-ZSM-5, are highly effective. Nickel acts as a hydrogenation site, while the zeolite framework provides acid sites for the oligomerization process. The performance of Ni-ZSM-5 can be modified by varying nickel loading and the acidity of the zeolite to achieve the desired product distribution. Acidic β-zeolites have also shown considerable activity in facilitating the oligomerization of olefins and producing hydrocarbons with high selectivity in the kerosene range [85,86].
iii) The final step, which is the hydro-processing step, includes hydrocracking and hydro-isomerization of the produced hydrocarbons, which refines the product into kerosene having the desired properties. Catalysts such as sulfided Co-Mo and Ni-Mo supported on alumina are commonly used for the hydrocracking process. These catalysts can effectively saturate the olefins and crack heavier hydrocarbons, ensuring a clean product with high kerosene yield. Hydro-isomerization, often catalyzed by bi-functional catalysts such as Pt/zeolite or Pd/zeolite, which introduce the branching in hydrocarbon chains, hence improving the cold flow properties. The activity and selectivity of these catalysts depend on the balance between their active metal and acidic sites, which can be modified to meet specific product requirements [87]. Different key catalysts and their features are shown in Table 4.

Advancements in catalyst design are driving improvements in this process. Controlling catalyst acidity reduces side reactions, while optimized pore structures improve the diffusion of intermediates. Enhanced metal dispersion on supports further boosts hydrogenation efficiency, making the process more effective for industrial applications. Catalysts are at the core of the MTK process, enabling the conversion of methanol into kerosene-range hydrocarbons. Ongoing innovations in catalyst development, such as zeolite modifications and new bifunctional designs, will be critical to improving efficiency and supporting SAF production.

3.3. Reactor design for MTK process

Reactor design is at the basis of the MTK process, due to its direct influence on the efficiency, product yield, and operational stability of the conversion pathway. Each of the 3 steps presented in Section 3.2 needs specific reactor configurations optimized for the reaction requirements and the nature of the catalysts employed.

Fixed-bed reactors are widely utilized for the conversion of MTOs. These types of reactors have stationary catalysts, such as ZSM-5, and are designed to manage high temperatures and pressures. Fixed-bed reactors are preferred for their simple operation, toughness, and reliability. However, the use of such reactors is limited because of the heat transfer problem and potential hot spots that can lead to catalyst deactivation. Industrial implementations of fixed-bed reactors have shown consistent performance in converting methanol to light olefins, making them a vital in MTO technologies [88,92,95].

The other commonly used reactors are fluidized bed reactors, which are especially used for large-scale MTO and oligomerization processes. The fluidized nature of the catalyst particles guarantees the uniform heat distribution throughout the reactor, efficient mass transfer, and reduced temperature gradients, hence minimizing the risks of catalyst deactivation. These reactors are at an advantage, particularly where continuous operation and high product throughput are required. However, challenges such as catalyst friction and complex design requirements can cause operational and maintenance difficulties [89,90,92].

Slurry phase reactors are common in the hydro-processing stage, where hydrogenation and isomerization reactions occur. These reactors employ a liquid medium to disperse the catalysts, which enhances heat dissipation and ensures uniform reaction conditions throughout the reactor. Slurry reactors are particularly effective under high hydrogen pressures and temperatures, making them ideal for refining kerosene-range hydrocarbons. Despite these benefits, issues such as catalyst separation and recovery add complexity to their design and operation [89,93,94].

Table 4
Key catalysts used for oligomerization and hydro-processing in MTK processes, including their performance metrics

Catalyst	Process	Key features	Performance metrics	Refs.
ZSM-5	Oligomerization	Shape-selective zeolite, high acidity, and thermal stability	High olefin selectivity (> 80%); robust operation under high temperatures (350–500 °C)	[85,88,89]
Acidic β-Zeolites	Oligomerization	β-zeolite with enhanced acid site density and moderate pore sizes	Selectivity for kerosene-range hydrocarbons > 70%; operating pressure: 20–40 bar; conversion > 80%	[88,90]
Pt-Sn/zeolite	Oligomerization	High stability; synergistic effects between Pt and Sn for olefin polymerization	High olefin conversion, reduced deactivation rates	[88,91]
Ni-Mo/Al_2O_3	Hydro-processing	Bifunctional catalyst; active for hydrogenation and mild hydrocracking	High conversion rates (> 90%); effective in removing sulfur and nitrogen compounds	[89,91,92]
Co-Mo/Al_2O_3	Hydro-processing	Robust hydrogenation catalyst; resistance to deactivation	High aromatics saturation; selective for kerosene-range hydrocarbons	[93]
Pt/Al_2O_3	Hydro-processing	Noble metal catalyst; excellent hydrogenation and isomerization capabilities	Improved cold-flow properties; > 95% hydrogenation efficiency	[93]
Pd/SiO_2- Al_2O_3	Hydro-processing	Strong hydrogenation activity and moderate acidity	Enhanced hydrocarbon yield (> 85%); reduced aromatic content	[94]

MTK = methanol-to-kerosene.

The hydro-processing of kerosene-range hydrocarbons often requires advanced hydrogenation units combining hydrogenation and isomerization in a single step. These units utilize high-performance catalysts capable of selectively converting olefins to saturated hydrocarbons while optimizing the fuel's cold flow properties. The integration of advanced hydrogenation technologies improves product quality and compliance with aviation fuel standards. However, such units are capital-intensive and require careful operational controls [89,90,92].

Recent studies have estimated that reactors related costs represent a significant share of the MTK process capital investment, with Bube et al. [96] and Palizdar [75] reporting values around 50–55% of the total equipment or fixed capital cost based on detailed sizing and cost correlations, while Ruokonen et al. [97] found a lower share (~11%) due to the dominance of compressor costs in their configuration.

Different rector types with References are shown in Table 5.

3.4. Design of the methanol to kerosene plants

In this section 3 different plant flowsheets have been selected as illustrative examples of the different MTK plant schemes presented in the literature. Each of them is based on the methodology of various studies, showcasing distinct approaches for the MTK process modeling.

In the first flowsheet shown in Fig. 11, based on Atsonios et al. [98], methanol synthesized from CO_2 and H_2, is initially converted to light olefins in an MTOs reactor. The reaction sequence in this reactor involves the conversion of methanol to DME, followed by the conversion of DME to light olefins. The MTO reactor is modeled as a stoichiometric reactor (R-Stoic in Aspen Plus) operating at 450 °C and 2 bar, with product yields derived from Avidan [78]. After olefin synthesis, ethylene is separated from the heavier olefins using a distillation column and headed to an ethylene dimerization reactor, which operates at 50 bar and 25 °C according to [106]. The heavier olefins are separated into propene and butene via another distillation column. Propene is sent to a propene oligomerization reactor, operating at 270 °C and 40 bar, based on process conditions from [107]. Butene, the bottom product of the column, is mixed with the output from the ethylene dimerization reactor and fed into a butene oligomerization reactor, operating at 350 °C and 10 bar, with conditions taken from [108]. The oligomers formed in the propene and butene oligomerization reactors are mixed and sent to a hydrogenation reactor, where olefins are converted into their respective normal and iso-paraffins (alkanes) with a conversion rate of 90%. After hydrogenation, the alkanes are passed through a series of distillation columns. Light gases are separated and sent to an auto-thermal reforming reactor , while the desired products, diesel and jet fuel, are collected at the bottom of the columns. All distillation columns are modeled using the RADFRAC model in Aspen Plus, while the Peng-Robinson property method is applied throughout the MTK process.

The second flowsheet, shown in Fig. 12, is derived from the study by Ruokonen et al. [70], which provides detailed process modeling for synthesizing kerosene, gasoline, and diesel from renewable methanol. Methanol enters the process at atmospheric conditions and is first directed to the MTO reactor, still operating at 450 °C and 2 bar. Within this reactor, methanol is converted to DME and water, followed by the formation of light olefins and additional water. The reactor operates isothermally, with high-pressure steam produced to manage the heat generated. Also in this case, the reactor was modeled as a stoichiometric reactor (R-Stoic) with fractional conversion data sourced from Avidan [78]. Water is removed from the reactor effluent also using a decanter. Then ethylene is separated from the other olefins via distillation and directly used as a fuel for high-temperature heat generation (stream fuel gases in Fig. 12). Conversely, durene ($C_{10}H_{14}$) is separated from the main olefin stream in a subsequent distillation column and sent to a dedicated heavy gasoline treatment unit (hydroisomerization reactor in Fig. 12). The light olefins are oligomerized into heavier olefins in a MOGD (Methanol-to-Olefin Gasoline and Diesel)

Table 5
Summary of the reactor types, configurations, operating conditions, advantages, and disadvantages for MTK conversion

Reactor type	Configuration	Operating conditions	Advantages	Disadvantages	Refs.
Fixed-bed reactor	Catalyst-packed bed	High pressure (30–50 bar), temperatures 300–450 °C	Simple design, proven technology, scalable for industrial use	Poor heat management, limited to specific reaction rates	[70,88,98,99]
Fluidized-bed reactor	Suspended catalyst particles in fluidized gas	Moderate pressure, temperatures up to 500 °C	Enhanced heat transfer, uniform temperature, and flexibility in catalyst replacement	Complex operation and high energy demand for fluidization	[100–102]
Multitubular reactor	Parallel tubes with a catalyst bed	High temperatures (400–600 °C), high pressures (> 30 bar)	High thermal efficiency, optimal for exothermic reactions	Expensive construction, challenging maintenance	[70,88,101]
Slurry reactor	Catalyst slurry in a liquid or semi-liquid medium	Moderate temperatures (200–300 °C), low to moderate pressure	Superior catalyst utilization, effective for complex reaction pathways	Catalyst separation required, operational complexity	[100–103]
Microchannel reactor	Compact design with microchannels	High heat and mass transfer efficiency, high temperatures, and pressures, depending on reaction requirements	Enhanced control over reaction parameters, rapid scalability, and low catalyst loading	Cost-intensive setup, limited for large-scale applications	[99,100,102,104,105]

MTK = methanol-to-kerosene.

reactor, operating at 40 bar and 200 °C. The reactor product is fractionated into a series of distillation columns, producing LPG, gasoline, and middle distillates. The middle distillates comprising olefinic kerosene and diesel, undergo hydrotreating in a hydrogenation reactor to saturate the carbon double bonds. This reactor operates isothermally at 300 °C and 40 bar, based on the data from [109]. The hydrogenated paraffinic distillate is separated from excess hydrogen and further distilled to produce kerosene and diesel [116].

The third MTK plant flowsheet, shown in Fig. 13 and based on Bube et al. [100], also consists of dehydration, oligomerization, hydrogenation, and fractionation stages. Methanol is first fed into the MTO reactor to form raw olefins under operating conditions of 450 °C and 3 bar. The reaction data are based on various sources [110–114]. The MTO reactor is coupled with a regenerator reactor (not shown in Fig. 13) where fuel gases are burnt to generate energy. The raw olefins are quenched to remove water, washed with caustic soda to remove CO_2, and dried before entering the oligomerization reactor.

In the oligomerization reactor, the olefins are converted into hydrocarbons in the kerosene range at 500 °C and 3 bar, using data from Avidan and Ortiz-Espinoza [78,112]. The product is cooled and sent to a separator, where fuel gas by-products are removed. The liquid product is directed to a middle distillation column to maximize kerosene output (bottoms). Light gases and naphtha are separated from heavier hydrocarbons, with the majority of light gases recycled to the oligomerization reactor and a small portion purged to prevent accumulation. The bottom product is sent to a hydrogenation reactor operating at 300°C and 50 bar. After hydrogen recovery, the reactor output is fractionated to produce kerosene, diesel, and waxes.

3.5. *Different modeling approaches of MTK*

All the 3 flowsheets selected as representatives of MTK plants have in common 3 major sections, namely methanol dehydration to olefins, olefins oligomerization, and then hydrogenation. Some variants in terms of process layout can be found in the study of Ruokonen et al. [70], where a hydro-isomerization section of the heavy olefins (durene) was also included. Another difference is in the study of Atsonios et al. [98], where the oligomerization process of the light olefins is done in 2 separate reactors for the butene and propene, and also a dimerization reactor is used before the oligomerization reactors for ethylene dimerization. However, differences exist in the modeling of the unit operations used at various stages, as described in the following.

- MTO*s*: The modeling of the MTOs (dehydration) reaction is mostly taken from the early paper by Avidan [78], it is based on the UOP/Norsk Hydro MtO process in Bube et al. (2024) [84], where coke formation was also considered.
- *Water and CO_2 removal*: The authors also address water management, as a significant amount of wastewater is generated, which can be purified and reused for hydrogen production. In the study by Atsonios et al. [98], a simple flash separator is used to remove water from the light olefins. In contrast, Ruokonen et al. [70] employ both a flash separator and a decanter to enhance water separation. Meanwhile, Bube et al. [100] use a water quench column to remove water and a caustic wash column to separate CO_2 from the produced light olefins using caustic soda.
- *Separation of light olefins*: Atsonios et al. [98] use 2 distillation columns in series to separate ethylene, propene, and butene, which are subsequently sent to the oligomerization section. Fuel gases are not separated at this stage but are instead removed later in the product fractionation section and then sent to the autothermal reforming section. Ruokonen et al. [70] employ a distillation column to separate noncondensable light hydrocarbons from the light olefins, directing these gases to a high-temperature heat generation unit. Durene is separated from the olefin product in a subsequent distillation column and sent to a dedicated heavy gasoline treatment

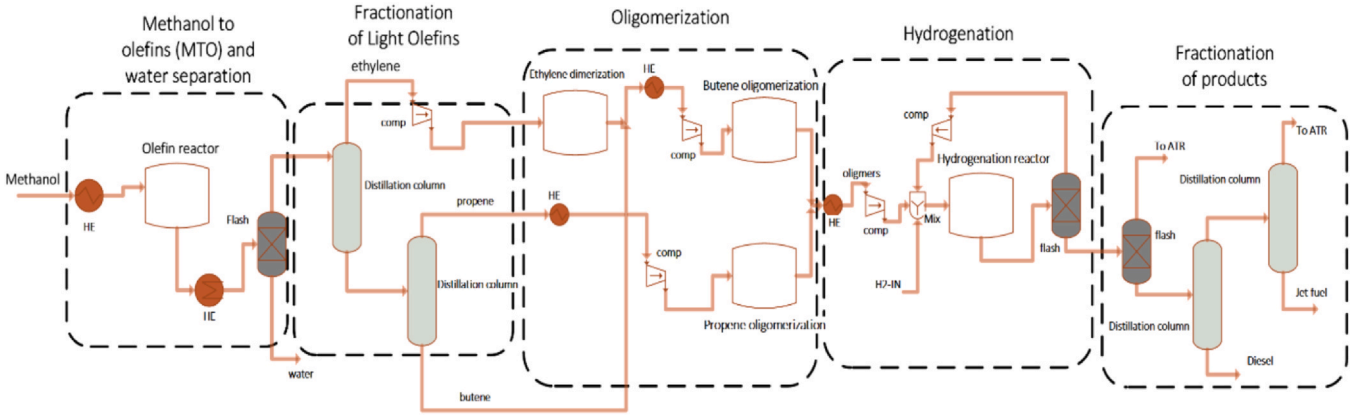

Fig. 11. Process flow diagram of MTK derived from Atsonios and coworkers' study [98]. MTK = methanol-to-kerosene.

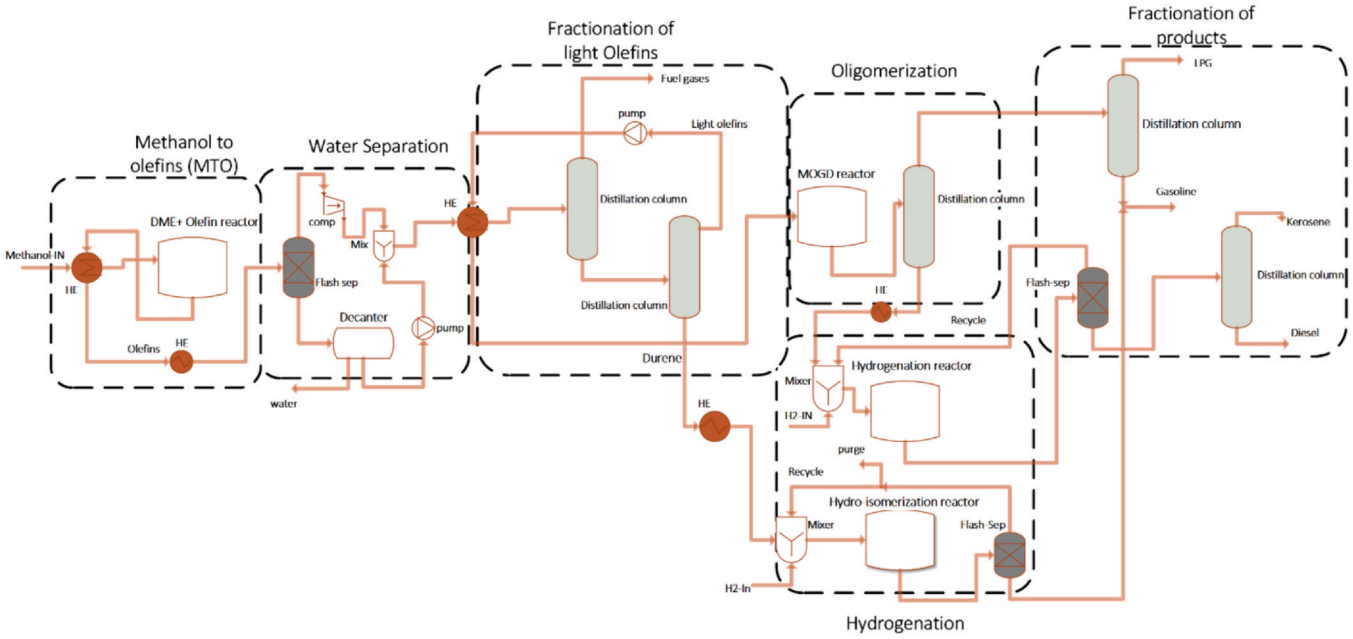

Fig. 12. Process flow diagram of MTK derived from Ruokonen and coworkers' study [71]. MTK = methanol-to-kerosene.

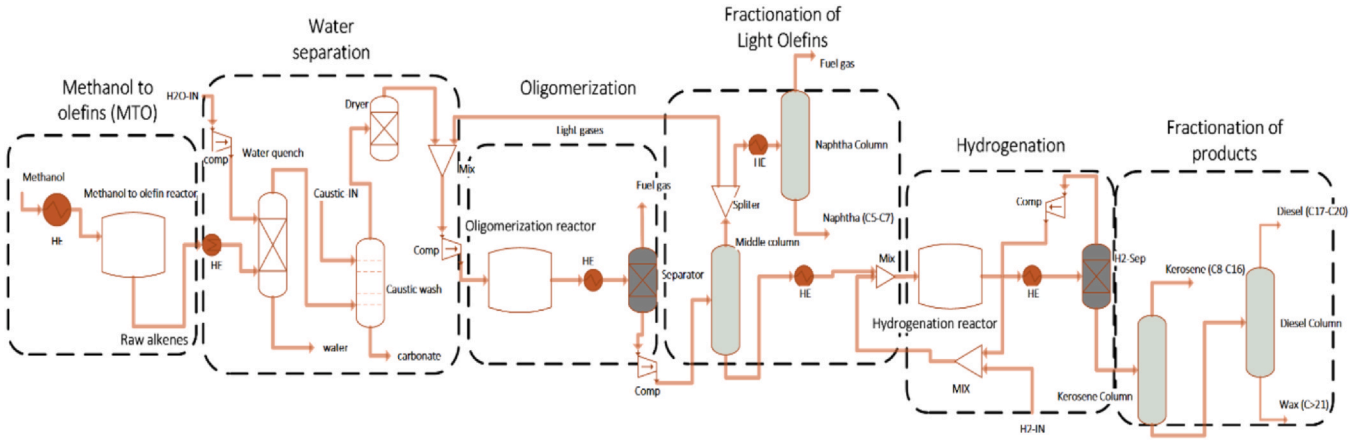

Fig. 13. Process flow diagram of MTK derived from Bube et al.'s study [101]. MTK = methanol-to-kerosene.

section. Bube et al. [100] conduct olefin fractionation after the oligomerization section, using 2 distillation columns to remove light MTO by-products, specifically light alkanes. To maximize the kerosene output, the bottom stream is fed into another distillation column (called the middle column), which further separates light gases and naphtha from the higher olefins.

- *Oligomerization reactors*: Atsonios et al. [98] utilize 3 separate reactors: one for ethylene dimerization to produce 1-butene, another

for butene oligomerization (mainly dimerization and trimerization), and a third for propene oligomerization to produce various oligomers (dimers, trimers, etc.). The oligomers are then mixed and sent to the hydrogenation section. The oligomerization reactors are modeled using R-Stoic, with reaction data for ethylene, propene, and butene oligomerization taken from references [106],[107], [108], respectively. Ruokonen et al. [70] use a single oligomerization reactor where light olefins are converted into heavier olefins. The MOGD reactor was modeled using a stochiometric reactor and adjusting the fractional conversion of each reaction to match the experimental data from Avidan [78]. Finally, Bube et al. [100] also used a single reactor for oligomerization but considered an Anderson-Schulz-Flory product distribution. [122]

- *Hydroprocessing reactors*: Atsonios et al. [98] employ a single hydrogenation reactor to process the mixed oligomers and convert them into alkanes. The hydrogenation reactor assumes 90% conversion of olefins into their respective n- and i-paraffins. Ruokonen et al. [70] use 2 separate hydrogenation reactors: one for the distillate blend (consisting of olefinic kerosene and diesel compounds from the oligomerization reactor) and another for the durene-rich aromatic gasoline fraction from the light olefin fractionation section. The hydrogenation reactor model follows the study reported in [109], with hydrogen feed estimated to be equimolar to the hydrocarbon flow, as suggested by Gang [115], and Ni/γ-Al_2O_3 as the catalyst. Bube et al. [100] use a single hydrogenation reactor modeled analogously to Fischer-Tropsch syncrude upgrading.
- *Fractional distillation*: Atsonios et al. [98] employ 2 distillation columns in series to separate the produced jet fuel, diesel, and light gases. Ruokonen et al. [70] first separate the excess hydrogen gas from the hydrogenation reactor output, followed by distillation to obtain kerosene and diesel. The hydrocarbon-hydrogen mixture from the hydrogenation of durene-rich olefins is further processed to recover 99.7% of hydrogen at 99.4 mol% purity, which is recycled to the hydrogenation reactor. Bube et al. [100] also use 2 distillation columns in series to separate kerosene, diesel, and wax.

3.6. Performance of the methanol to kerosene pathway

In this section, the performance reported in the literature for the MTK pathway is shown in different plots focusing on mass yields, energy efficiency, and carbon efficiency. Besides the 3 abovementioned studies of MTK, 3 additional studies have been added to obtain a more complete picture of the potential of the MTK pathway. Table 6, summarizes the primary purposes of these studies and the main co-products.

3.6.1. Mass yield

The MTK mass yield varies in a wide range between 9 and 36 wt% (Fig. 14), depending on the desired product slate, the hydrogen sourcing, and the recycling of light gases. In the following, this spread of yield values across different studies is explained in more detail.

The fuel product in Atsonios et al. [98] is composed of kerosene and a small fraction of diesel. Instead, the light fraction from the jet fuel fractionation column with shorter chain paraffins ($< C_9$, not suitable for jet fuel), which is unavoidably produced due to the selectivity towards light olefins at the oligomerization catalyst, is used as a fuel in the autothermal reformer for syngas production. Thus, in spite of the staged oligomerization process, the final kerosene yield (18.0 wt%) is modest.

The fuel product distribution in Eyberg et al. [101] shows that only 31.4% of the liquid hydrocarbon product is converted into jet fuel, since a significant fraction (45%) ends up in the diesel/waxes cut. This explains the low yield of MTK (9.2 wt%) compared to other studies, where the jet fuel fraction is maximized. On the other hand, the methanol to total liquid fuel product mass ratio (29.4 wt%) is even better than Atsonios et al. [98] because gasoline also contributes to the final products. [71] The yields in Ruokonen et al. [70], albeit slightly higher in value, follow the same trend as in Eyberg et al. [101], with the jet fuel cut

Table 6
Main fuel products and co-products considered in the different studies on MTK plants

Primary purpose of the plant	Main fuel product	Other useful fuel products	Note	Refs.
Production of kerosene	Kerosene	Gasoline/naphtha and diesel	Recycle of light olefins to the oligomerization reactor	Bube et al. [100]
		Gasoline and diesel	Recycle of light olefins to the oligomerization reactor	Voß et al [92]
		Diesel	The gasoline fraction is used as a fuel in the ATR	Atsonios et al. [98]
Production of liquid fuels, including kerosene		Gasoline and diesel/waxes	Low selectivity in kerosene	Eyberg et al. [101]
		Gasoline and diesel	Low selectivity in kerosene	Ruokonen et al. [70]

ATR = Auto-Thermal Reforming; MTK = methanol-to-kerosene.

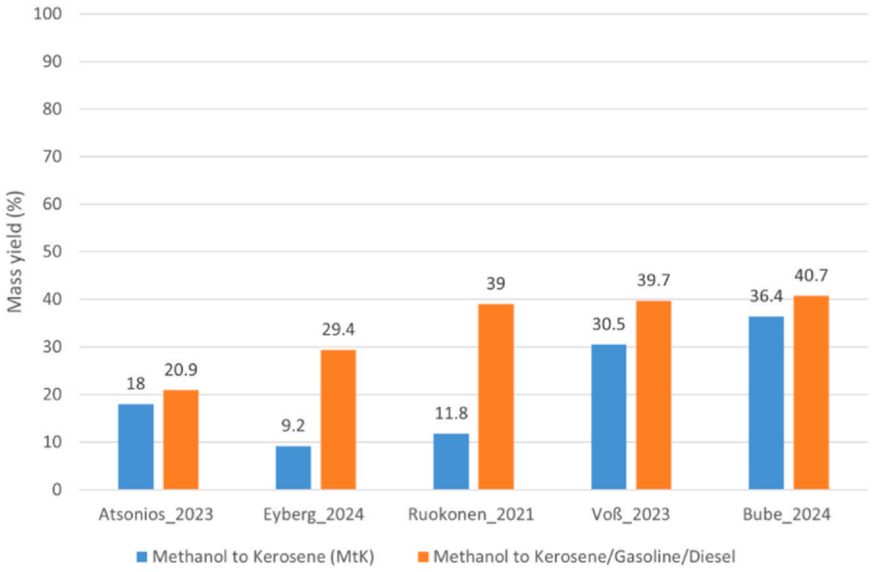

Fig. 14. Mass yield of methanol to kerosene (blue bars) and mass yield of methanol to all liquid fuel products (orange bars) reported by different authors.

representing approximately one third of the total fuels.

The newer studies show higher selectivity towards the jet fuel cut. In Steffen Voß et al. [92], the MTK mass yield (inferred from the energy balance) has been calculated to be equal to 30.5 wt%, which is roughly 2-3 times higher compared to the previous studies. Similarly, in Bube et al. [100], the maximum MTK yield reached 36.5 wt%. On the other hand, the mass yield of the total fuel product in both cases is limited to 40–41%, which is consistent with Ruokonen et al. [70].

To further expand on these values, Fig. 15 shows the percentage fraction of kerosene compared to all liquid fuel products. It clearly appears that the MTK process can achieve remarkable kerosene fractions approaching 90% (like in Bube's work), depending on catalyst selectivity and optimization of the process [100,116]. The high selectivity toward kerosene fractions is assisted and could be further enhanced by advanced catalytic systems such as solid phosphoric acid catalysts and zeolites, which can improve the distribution of hydrocarbons toward the range of jet fuel [70,104].

3.6.2. Chemical energy efficiency

The chemical energy efficiency, defined as the ratio between the energy content of the product/s stream and the energy content of the methanol stream, is shown in Fig. 16. As expected from the mass yield results, the maximum values of MTK energy efficiency are those reported in Bube et al. [100] and Voß et al. [92], whereas lower values are reported by the other authors. By including the energy value of the co-products (gasoline and diesel), the chemical energy efficiency is similar for 3 out of the 5 studies in Fig. 18. The differences are ascribable to different integrated thermodynamic optimization of key processes, staged oligomerization of the olefins [98,101], and recycle of light gases.

The moderate MTK chemical energy efficiency (33.6%) in Atsonios et al. [98] is consistent with the mass balance results, since a significant fraction of hydrocarbon products is composed of lighter hydrocarbons that are used internally for syngas production. On the other hand, in Eyberg et al. [101], the low MTK energy efficiency (20.0%) is the result of the poor selectivity in kerosene, as already mentioned above, which results in high fractions of energy associated with the gasoline and diesel/waxes cuts. In Ruokonen et al. [70], the higher energy efficiencies for both kerosene and total fuels compared to Eyberg et al. [101] are consistent with the higher yields.

Higher MTK energy efficiencies can be seen in the newer studies. In Bube et al. [100], the MTK energy efficiency reaches the remarkable value of 72.9%, which is the highest among the studies considered here. This is the main outcome of the light olefin recycle from the top of the

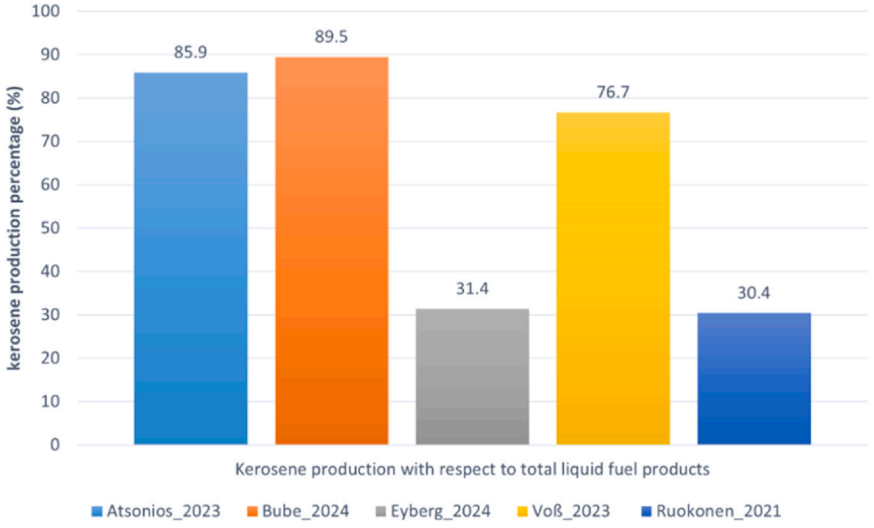

Fig. 15. Share of kerosene compared to total liquid fuel products (gasoline, jet fuel, diesel).

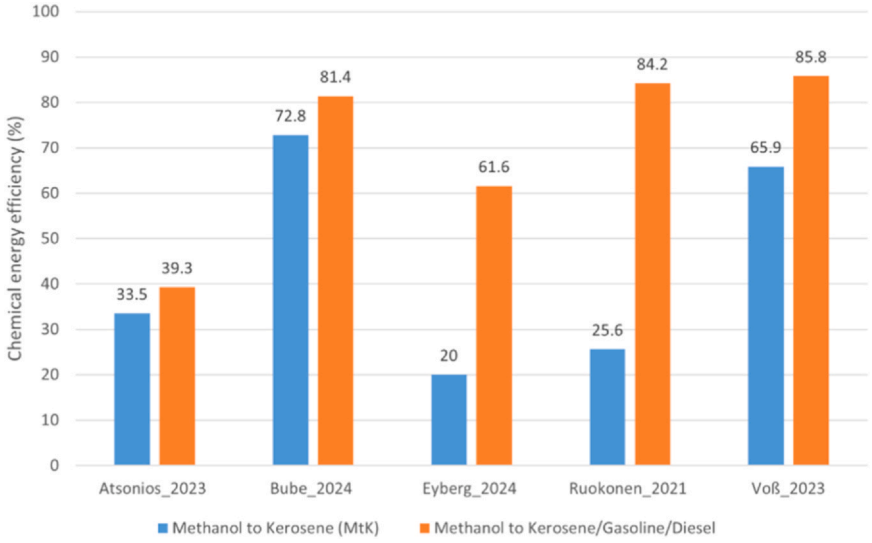

Fig. 16. Chemical energy efficiency of methanol to kerosene (blue bars) and methanol to all liquid fuel products (orange bars). HHV basis for Atsonios (2023) and Bube (2024), and LHV basis for Eyberg (2024), Ruokonen (2021), and Voβ (2023). HHV = Higher Heating Value; LHV = Lower Heating Value.

middle column to the oligomerization reactor, which maximizes the yield of kerosene to the detriment of the gasoline/naphtha output. Similarly, in Steffen Voß et al. [92] a MTK energy efficiency of 66.0% has been calculated due to the higher selectivity towards the kerosene fraction that is achieved through recycle of the lighter components. In both cases, the energy efficiency for the total fuel products is in the range 81–86%, which is consistent with Ruokonen et al. [70], where a wider spectrum of useful fuel products was considered.

3.6.3. Carbon efficiency

The carbon efficiency values shown in Fig. 17 also aligns with the energy performance. The maximum carbon efficiency is 78% (Bube's work) when focusing on methanol only, while it reaches 94% (Ruokonen's study) when considering all the liquid fuel products. The difference in carbon efficiency values is related to more or less effective recycling of light gases and strategic process integration.

In the study by Voß et al. [92], the MTK carbon efficiency was 59%. Indeed, the carbon content in methanol represented 31.9% of the total carbon originally present in corn stover, and after conversion into long-chain hydrocarbons, the carbon content in the kerosene fraction was 18.9%. The carbon losses in MTK resulted from a broader oligomerization distribution, as single-step oligomerization was chosen, and due to the formation of short-chain alkanes and CO_2 by-products from the MTOs plant. In the study by Ruokonen et al. [70], carbon efficiency reaches up to 94% as almost all methanol is converted into valuable products, with a similarly high energy efficiency. In the study by Eyberg et al. [101], the maximum carbon efficiency for methanol-to-jet fuel is achieved in the light gas recycle (LGRC) case.

According to the study by Bube et al. [100], during the upstream process (methanol production), carbon efficiency is almost 98%, with purge gases being the only significant losses. However, major carbon losses occur in the downstream MTK process. During methanol dehydration, about 3% of carbon is discharged as coke, which is subsequently released as CO_2 during catalyst regeneration. Additionally, carbon losses in the oligomerization process range from approximately 3–7%, due to the removal of light alkanes as purge gases from separators and the purging of inert components from the middle column. Carbon losses also occur due to heavy components like wax, which are utilized as fuels in furnaces.

3.7. Challenges in the MTK pathway

The conversion pathway MTK entails several critical challenges which are partially shared with MTG, as summarized in the following:

- *Process Efficiency and Energy Requirements*: The MTK conversion process includes several steps, each of them requiring specific

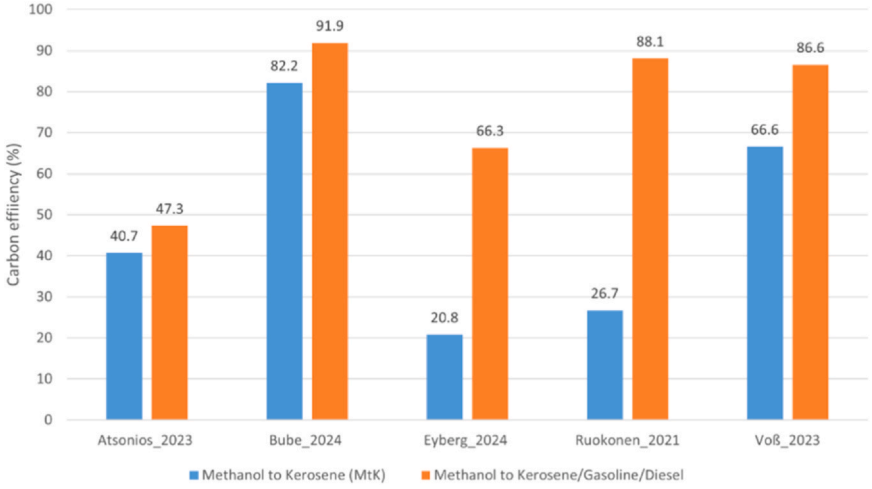

Fig. 17. Carbon efficiencies for MTK processes reported by different authors. MTK = methanol-to-kerosene.

energy and thermal conditions. Reactions such as olefin oligomerization require high temperature and high pressure conditions, which cause high operational energy demands [98,99]. Additionally, optimizing the heat integration and recycling the by-products into the system to improve energy efficiency remains a considerable technical challenge [100,101].

- [104,109,110,125] *Catalyst Stability and Performance*: Catalyst deactivation due to coking, fouling, and sintering at high temperatures is a major issue, particularly for catalysts used in dehydration and oligomerization [117]. Furthermore, achieving high selectivity for kerosene range hydrocarbons is difficult, as side reactions often produce lighter products like gasoline as well as heavier waxy by-products [118]. Additionally, developing aromatics-free kerosene to minimize non-CO_2 aviation emissions is a recent challenge that requires innovative catalytic processes [105].
- *Economic Viability*: The process is significantly more expensive than traditional fossil-based kerosene production due to the high costs of renewable inputs like green hydrogen, renewable energy, and CO_2 capture [93,119]. Without substantial subsidies or the implementation of carbon taxes, MTK pathways struggle to compete with fossil kerosene in terms of market competitiveness [90,95,105,108].

Research efforts are ongoing to address all the abovementioned challenges, which are driven by the highly encouraging environmental implications. Indeed, life cycle assessment studies suggest that MTK-derived SAF can reduce GHG emissions by up to 85 percent to 90 percent compared to fossil jet fuel, depending on the renewable energy share in the input streams [88,103].

4. Economic analysis of the MTG and MTK pathway

The results of the economic analyses carried out for both MTG and MTK pathways in the literature are summarized in this section, focusing on the methanol to the final product (either gasoline or kerosene) conversion step. The cost of gasoline and kerosene production from methanol is primarily determined by the capital expenditures (CAPEX) and operational expenditures (OPEX) associated with methanol conversion. CAPEX includes the costs associated with the equipment, materials, and installation, whereas OPEX covers day-to-day expenses such as raw materials, salaries, utilities, rent, and maintenance.

4.1. Methanol-to-gasoline (MTG) economic analysis

In the following, the research methods and most significant findings obtained from selected economic studies on MTG are briefly summarized.

An economic analysis of gasoline production from methanol was conducted in Arias Gallego et al. [64] using different Aspen software tools (Energy Analyzer and Economic Analyzer). Hydrogen needed in the hydro-processing section was assumed to be priced at 1500 $/ton [43]. Additionally, methanol prices varied between 150 $/ton and 1000 $/ton depending on the source (gray or green methanol) [120,121], significantly impacting the levelized price of e-gasoline. Using gray methanol as the feedstock at 250 $/ton, the levelized cost of e-gasoline was calculated at 1.82 $/L. A break-even point was reached in the eighth year, after which the plant began generating profits. Instead, using green methanol at the current 2020s prices (750–1000 $/ton), the levelized cost of e-gasoline was calculated in the range 2.8–3.5 $/L, which is roughly 1.5–2 times higher than using gray methanol. With the expected reduction of green methanol price in the near future, the foreseen price for MTG gasoline in the 2030s was estimated around 2.3–2.4 $/L.

Targeting the reduction of production costs, some authors focused on the production of gasoline from bio-methanol. For instance, Phillips et al. [58,122] conducted a similar economic analysis for gasoline and LPG production obtained from woody biomass-derived methanol for a plant capacity of 2000 dry metric tons of biomass per day. Using poplar woody biomass priced at 55.89 $/dry metric ton, the estimated plant gate price of gasoline and LPG was 15.37 $/GJ (0.52 $/L) in 2007 US dollars. The study identified feedstock cost as the primary contributor to the price of gasoline, with catalyst costs having a negligible impact. In the study of Hennig and Haase [59], the economic analysis focused on the production of gasoline from methanol obtained from biomass-derived syngas enriched with green hydrogen [123]. The cost of residual straw was assumed equal to 83.9 $/ton, whereas the cost of hydrogen was assumed quite high, approaching 10 $/kg. The total product cost (TPC) was calculated in the range of 2.98–3.06 $/L of fuel depending on on-site/off-site hydrogen production. Among the different costs, raw materials (hydrogen and straw) made the largest fraction of the TPC, having a total share of 75%, with the cost of hydrogen having the single largest fraction. The authors concluded that the green hydrogen enhancement technique could become competitive only at hydrogen prices below 3.2 $/kg.

Other authors considered combinations of fossil fuels and biomass. Baliban et al. [124] analyzed gasoline production using a hybrid combination of coal, biomass, and natural gas, estimating liquid fuel (gasoline, diesel, and kerosene) costs between 0.54 $/L and 0.59 $/L for a 10,000-barrel-per-day (10 KBD) plant. Scaling up to 50 KBD reduced costs to 0.49–0.55 $/L, while a 200 KBD plant had costs between 0.45–0.50 $/L. When the plant production targets only gasoline and diesel (i.e., no kerosene), the cost for each capacity decreases by about 0.01 $/L, due to the decrease in investment needed for the fractionation process.

The prices of gasoline obtained in MTG processes by different authors are shown in Table 7.

4.2. Methanol-to-kerosene (MTK) economic analysis

The methods and most significant findings obtained from the economic studies on MTK are briefly summarized in the following.

The economics of MTK plants were assessed in Ruokonen et al. [78] based on the developed MTK flowsheet modeling and using the Aspen Process Economic Analyzer tool. Interestingly, compressors accounted for 75% of the total equipment costs, with reactors and distillation columns contributing to most of the balance. Additional costs, such as engineering and design, significantly increased overall expenditures. The variable costs represented the majority of the total cost of production, with the green methanol cost of 0.91 $/L accounting for approximately 70% of the annual expenses. Catalyst replacement was assumed every 2 years [49], since lifetimes vary between 1.5 and 3 years [125]. The total production cost for the liquid transport fuels was calculated equal to 3.25 $/L, which was deemed too high compared to the average fossil fuel price of 1.11 $/L.

By extending the analysis to the green methanol production process, Eyberg et al. [101] conducted an economic analysis of e-kerosene production from CO_2 and H_2, where CO_2 was obtained using a DAC system, while H_2 was generated in a high-temperature solid oxide electrolyzer (SOEL). The plant product was a mixture of liquid hydrocarbons, leaving the fractionation section out of the scope of the analysis. They found that SOEL cost accounted for the major fraction in the total investment cost, with a share of 59–67%, while the DAC cost share was about 15–20%. As a consequence, the production costs ascribable to the methanol synthesis stage were found to be higher than those attributable to the MTK conversion stage. The levelized cost of production of e-kerosene in the most efficient layout (named MTJ-LGRC) that included an LGRC, was calculated to be equal to 8.43 $/L, i.e., 9 times higher than the average cost of fossil jet fuel in 2022. The price of electricity and the electrolyzer capital investment were identified as the key factors in high production costs. Even in a future scenario at 2050 with cheaper renewable electricity and established DAC and SOEL technologies, the foreseen production cost was estimated to be still

Table 7
The product cost of synthetic gasoline produced in MTG processes from different feedstocks

Source of methanol	Methanol product cost($/L)	Cost of synthetic gasoline ($/L)	Year U.S. dollars	Refs.
Natural gas (gray methanol case)	0.198	1.82(potential reduction to 0.76 with increased plant capacity)	2023	Arias Gallego et al. [57]
Green hydrogen and CO_2 or syngas frombioenergy (green methanol case)	0.594–0.792(potential reduction to 0.396 at 2030s)	2.85–3.50(potential reduction to 2.75 at 2030s)	2023	Arias Gallego et al. [57]
Woody biomass (hybrid poplar wood chips)	N.A.(only the cost of dry biomass is given, which is 55.9 $/ton)	0.520(plant gate price at baseline conditions)	2007	Phillips et al. [122] and NREL report [58]
Waste agricultural biomass (residual straw)	N.A.(only the cost of dry biomass is given, which is 83.9 $/ton)	2.98–3.06[a] (total product cost)	2018	Hennig and Haase [59]
A combination of coal, biomass, and natural gas	N.A.	0.453–0.591(depending on plant capacity)	2009	Baliban et al. [124]

MTG = methanol-to-gasoline; NREL = National Renewable Energy Laboratory.
[a] Calculated from the reported total product cost, assuming a product density of 0.8 kg/L and a currency exchange rate in 2018: 1 € = 1.1810 $.

high, around 2.39 $/L. On the same page, Schmidt et al. [88] analyzed PtL jet fuel economics, considering the costs for the mid 2010s and those projected for the year 2050. Both high and low temperature electrolysis technologies were assessed, and both direct capture from air or a concentrated biogenic CO_2 source were considered. The cost of renewable electricity from solar and wind was assumed to be 10.3c €/kWh in the mid-2010s scenario, and it dropped to 4.0c€/kWh in the long term scenario. From the study, it was evident that the cost of renewable power was the main driver for the PtL production cost; the DAC process for CO_2 production showed a great impact as well. Indeed, the cost of jet fuel was calculated to be equal to 2.77 $/L for the concentrated CO_2 source, while it reached 3.71 $/L for integration of a DAC system. In the year 2050, these costs could be reduced to approximately 40%.

Aiming at the abatement of the production costs, the economic analysis in Voß et al. [92] focused on a hybrid biomass- and PtL-based kerosene production concept, which might offer potential advantages in terms of yield and carbon efficiency. In the hybrid ethanol-to-kerosene plant, corn stover was used to produce ethanol, which was dehydrated and combined with the light olefins from the MTO reactor. Instead, in the hybrid biogas to kerosene process, the reforming of biomethane produced part of the gas feed to the methanol reactor. In both the hybrid plants, the total kerosene production cost was 2.34 $/L, where the purchase of electricity accounted significantly. Indeed, the production cost of the biogenic-derived e-kerosene portion was found to be much lower than that of the electrically derived portion.

The prices of methanol-derived kerosene calculated in different studies are shown in Table 8.

4.3. Improving the economics of MTG and MTK

The options suggested in the literature to abate the price of e-gasoline and e-kerosene are various: i) the increase of plant capacity to several thousands of barrels per day [22,23,57,88,124]; ii) the introduction of new green methanol technology with the potential of halving its production costs in the next 10 years [57]; iii) the further research and development of MTG reactors such as the use of fluidized bed MTG reactor [58,122]; iv) a better valorization of the light hydrocarbon fraction and other co-products [58,122]; v) the drastic reduction of the cost of renewable electricity and green hydrogen [22,59,88]; vi) the long term projected cost reductions for DAC and solid oxide electrolysis [101]; vii) a reduction in hydrogen consumption in the upgrading process; viii) the recovery of valuable chemicals such as benzene, toluene and xylene [59]; ix) the use of hybrid biomass-PtL systems [92]; x) the development of novel integrated plant configurations with multiple products [75,76]; xi) much higher carbon taxes on CO_2 emissions from fossil fuels compared to those currently applied [101]; xii) an increased awareness by the consumers to accept an increase of fuel prices when obtained from renewables [101]; xiii) incentives or tax exemptions when using renewable fuels [70,97]; xiv) binding emission reduction targets for the transport sector [70,97]. Only an effective combination of these strategies will allow e-gasoline and e-kerosene to be competitive against their fossil counterparts.

5. Comparison between MTG and MTK processes

5.1. Process design

The MTG and MTK processes differ significantly in terms of process design, primarily because each pathway targets a different final product and involves distinct catalytic and operational steps.

In the MTG process, methanol is first dehydrated to DME using a mildly acidic oxide catalyst such as γ-Al_2O_3 at 440°C and 10 bar. This reaction is exothermic, and the heat generated helps balance the overall thermal energy requirements of the process. The produced DME then passes through a series of catalytic reactors, where zeolite ZSM-5 serves

Table 8
Product cost of kerosene from different MTK studies

Source of methanol	Methanol price	Cost of kerosene US $/L	Year dollars	Refs.
PtL (CO_2 from DAC and H_2 from SOEL)	N.A	8.43 $/L[a](liquid hydrocarbon products)	2022	Eyberg et al [101]
PtL (H_2 from alkaline electrolyzer and CO_2 from concentrated source)	0.91 $/L	3.25 $/L (total product cost)	2020	Ruokonen et al [70]
PtL (H_2 from alkaline or PEM electrolyzers and CO_2 from DAC or concentrated source)	N.A	3.71 $/L (DAC)2.77 $/L (concentrated CO_2 source)	2017	Schmidt et al [88]
Hybrid biomass and PtL (concentrated biogenic CO_2, and H_2 from alkaline or PEM electrolyzer)	N.A	2.34 $/L (for both hybrid plants)	2022	Steffen Voß et al_2024 [92]

DAC = direct air capture; MTK = methanol-to-kerosene; PtL = power-to-liquid; SOEL = solid oxide electrolyzer.
[a] Calculated from the reported value of 0.81 €/kWh, assuming an average heating value and density of the total hydrocarbon products equal to 44 MJ/kg and 0.8 kg/L, respectively.

as the catalyst. Within these reactors, methylation, cracking, and aromatization reactions convert DME and unreacted methanol into hydrocarbons in the gasoline range. The process achieves high selectivity (~80%) for gasoline, with LPG as a by-product. After gasoline production, a distillation unit removes light gases and heavy aromatic compounds. The final refining step involves hydro-isomerization, which enhances fuel quality by improving the octane rating and reducing sulfur content. This type of process design has been implemented in commercial-scale gasoline production plants, such as Mobil's facility in New Zealand, with continuous advancements for improved scalability and efficiency.

On the other hand, the MTK process is designed to produce heavier distillates. This process occurs in several steps. First, methanol is converted into light olefins in the MTO reactor at 450°C and 2 bar. In the second step, the produced light olefins undergo an oligomerization reaction in a separate reactor, which is designed in a way that the conversion of propene and butene into heavier hydrocarbons occurs. After the oligomerization process, the produced heavy hydrocarbons are headed to the hydrogenation section, where they are converted into paraffins and iso-paraffins. At the end, a series of distillation columns separates the produced LPG, gasoline, kerosene, and diesel fractions. The MTK process consists of various distinct steps for the separation and hydrotreatment of the produced fuel, aiming to produce high-quality kerosene and diesel for the aviation and industrial sectors.

In conclusion, the MTG process is comparatively simpler than the MTK process, because it includes dehydration of the methanol, which is followed by the conversion of hydrocarbons into gasoline-range hydrocarbons. On the other hand MTK process is more complicated, requires a series of steps for the oligomerization, hydrogenation, and distillation to produce the kerosene and other distillates.

5.2. Catalysts

In the MTG pathway, the role of the catalyst plays a crucial role in determining the process efficiency, product yield, and selectivity of the product. Different catalysts have been used in the MTG process, but the ZSM-5 zeolite-based catalyst is one of the best due to its shape-selective microporous structure, which helps the formation of gasoline-range hydrocarbons while minimizing unwanted by-products. Among the different advantages of using ZSM-5 catalyst, one of the key advantages is its high thermal stability, which increases its lifetime and makes it economically viable for industrial applications. Further improvements in ZSM-5-based catalysts, such as CuO/HZSM-5 and ZnO/HZSM-5, can enhance catalytic performance by improving hydrogen transfer reactions and reducing coke formation during the process, hence increasing paraffin yield and stabilizing the produced olefins. Coke deposition, which is one of the main reasons for catalyst deactivation, can be minimized by optimizing the Si/Al ratio in ZSM-5, and to improve the octane number of gasoline, the selectivity of the catalyst towards aromatics can be adjusted. Furthermore, ZSM-5 and its modified catalyst versions can ensure the production of sulfur and nitrogen-free gasoline, aligning with environmental regulations.

A more complex catalytic system is required in the MTK pathway due to the multistep conversion process. During the first step, which involves the conversion of methanol into light olefins, the most commonly used catalyst is H-ZSM-5, which is chosen due to its strong acidity and thermal stability, which facilitates the effective conversion of methanol into light olefins such as ethylene and propylene. In the succeeding oligomerization step, nickel-based catalysts such as Ni-ZSM-5 are utilized. The final step, which is the hydro-processing stage, requires bi-functional catalysts such as Ni-Mo/Al_2O_3 or Co-Mo/Al_2O_3, which are highly effective for hydrogenation and mild hydrocracking, leading to the production of clean, high-yield kerosene. These catalysts also help in removing the sulfur and nitrogen compounds, which improves the quality of the produced kerosene. Moreover, catalysts like Pt/zeolite and Pd/zeolite are used for the hydro-isomerization process

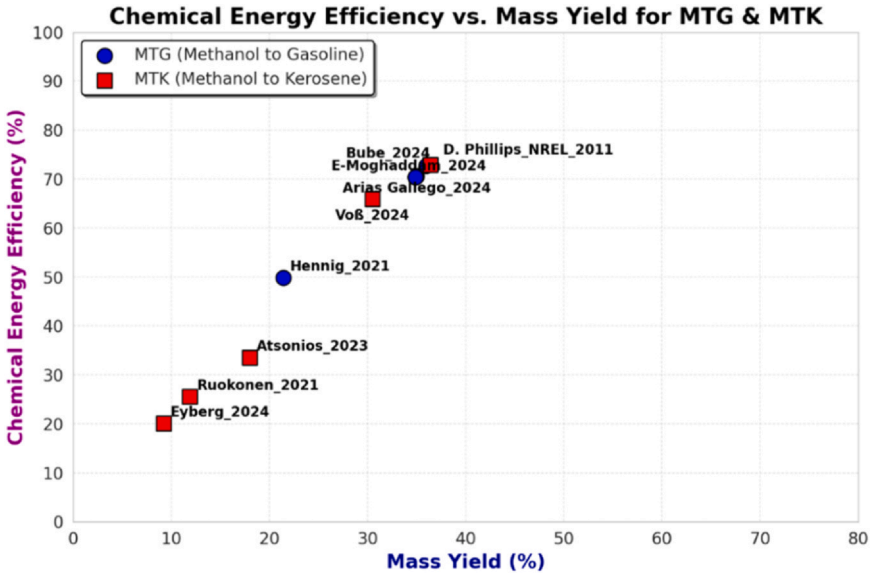

Fig. 18. Comparative plot showing chemical energy efficiency versus methanol to product mass yield for both MTG and MTK processes. MTG = methanol-to-gasoline; MTK = methanol-to-kerosene.

to improve the cold flow properties of kerosene by introducing branching in hydrocarbon chains.

5.3. Performance

The chemical energy efficiency versus mass yield chart shown in Fig. 18 compares the values reported in the literature for the MTG and MTK pathways. Broadly speaking, the MTK performance results (red squared marks) mostly lie on the bottom left-hand side of the chart, whereas the MTG results (blue circles) mostly lie on the upper right side. This demonstrates that the selectivity of the methanol conversion process and the resulting chemical energy efficiency are better for the MTG compared to the MTK. Even though the most recent studies on MTK, e.g., by Bube et al. [100], show the possibility of improving both metrics, the MTK performance still falls short of MTG.

The results reported in the carbon efficiency – mass yield chart shown in Fig. 19 are consistent with those of the energy efficiency chart. The MTG process can achieve remarkable carbon efficiency values even slightly exceeding 80%, which currently appears unattainable by the MTK pathway. Also in this case, the recent investigation by Bube et al. [100] reports the possibility to improve the carbon efficiency up to around 80%.

5.4. Economics

In terms of economics, the following comparison can be drawn. MTG and MTK processes are significantly different in their cost structures.

According to the economic analysis by Arias Gallego et al. [57], a typical MTG plant using gray methanol as the feed results in a levelized cost of synthetic gasoline of 1.82 USD per liter, which increases up to 2.85–3.5 USD/L using green methanol. Similar to MTG, the economics of the MTK process are also affected by the high CAPEX and OPEX, but it also encounters different challenges and cost drivers. On the other hand, the e-kerosene costs reported in Schmidt et al. [88] are equal to 2.77–3.71 $/L, which appear quite aligned to those of e-gasoline in spite of the higher plant complexity. [71]

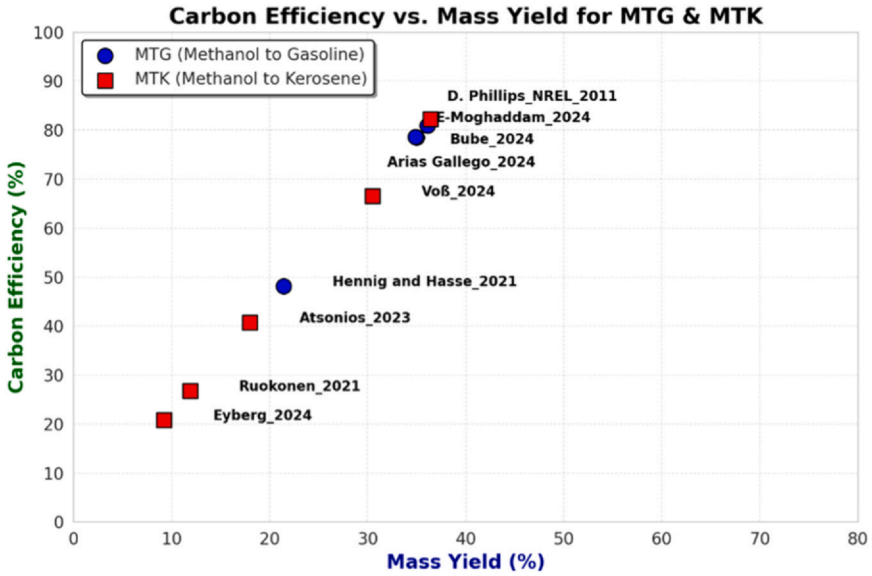

Fig. 19. Comparative plot showing the methanol to product carbon efficiency versus mass yield for both MTG and MTK processes. MTG = methanol-to-gasoline; MTK = methanol-to-kerosene.

Both the MTG and MTK processes depend heavily on green methanol as the feedstock, with its cost being a key factor in overall production expenses. Accordingly, the differences in the methanol to product conversion stage appear less relevant when considering the economics of the overall plant.

6. Conclusion

The transition towards sustainable transport fuels is requisite to achieve GHG reduction and fulfill global climate aims. This review has systematically analyzed and compared the 2 technologies known as MTG and MTK, considering the process designs, catalysts, reactor types, performance, energy efficiency, and economics. Both routes offer potential alternatives to fossil fuels to meet the increasing demands for renewable road and aviation fuels.

The MTG process shows a remarkably high gasoline selectivity (close to 90%) with ZSM-5 catalysts, and is considered a good candidate for production of e-gasoline (as compared to the FT-based processes) for light-duty vehicles. The reported MTG yields are aligned around 35–36 wt%, which reach 40–41 wt% when including the LPG co-product. Consequently, the chemical conversion efficiency reaches high values in the range 70–73%, which rises up to 88% when considering the LPG energy. Moreover, the electrical and thermal energy demands are generally moderate. Thus, the high-energy thermodynamic efficiency combined with the compatibility with the current fuel infrastructure (i.e., the gasoline engine), and the proven industrial viability of the MTG production plants continue to make this pathway of interest for further deployment.

The newer MTK process also demonstrates good prospects for synthesizing SAFs from methanol in this hard-to-electrify sector. The 3-step catalytic method based on MTOs, oligomerization, and hydro-processing, even though more challenging than MTG, provides a highly effective synthesis of kerosene-range hydrocarbons. The MTK mass yields have been found highly variable in the range 9–36 wt%, where the highest values are achieved only in the most recent studies, maximizing the selectivity towards the kerosene product. The corresponding chemical energy efficiency has been found in the range 20–73%, which demonstrates the possibility to achieve similar figures as in the MTG process. On the other hand, the MTK process is characterized by a higher energy demand, as clearly visible by the higher number of compressors, distillation columns, and reactors, as well as by a higher hydrogen demand compared to MTG.

With regards to the economics, it can be concluded that there are some factors, such as the source of hydrogen and carbon dioxide for e-methanol synthesis, which exceed by far the MTG-MTK differences in the conversion process costs and efficiencies. Thus, the higher product costs resulting from the additional complexity and lower yield of the MTK plant must be commensurate in the context of the wider energy system, where the production cost of e-methanol is currently representing the most critical factor. Newer methods, such as direct electrolytic methanol synthesis, are beginning to appear at lab/pilot scale level and could soon represent the enabling factor for the uptake of the MTG and MTK technologies.

In summary, this work presents a systematic comparison of MTG and MTK pathways, addressing a clear gap in the literature where most prior studies have focused on a single route. By juxtaposing these pathways, we have not only identified their individual bottlenecks but also uncovered opportunities for synergy. Shared methanol infrastructure, integration into existing refinery operations, and cross-learning in catalyst and reactor optimization can collectively accelerate commercialization. Thus, rather than viewing MTG and MTK as alternative routes, this study underscores their potential complementarity in a diversified low-carbon fuel portfolio for both road and aviation sectors.

Declaration of Competing Interest

The authors declare that they have no known competing financial interests or personal relationships that could have appeared to influence the work reported in this paper.

Declaration of Generative AI and AI-assisted technologies in the writing process

During the preparation of this work, the author used Grammarly to review spelling, grammar clarity, and delivery mistakes in English. After using these tools and services, the author reviewed and edited the content as needed and takes full responsibility for the content of the publication.

Acknowledgments

This work has been supported under the National Recovery and Resilience Plan (NRRP), Mission 4 Component 2 Investment 1.4 - Call for tender No. 3138 of December 16, 2021 of the Italian Ministry of University and Research, funded by the European Union - NextGenerationEU [Award Number: CNMS named MOST, Concession Decree No. 1033 of June 17, 2022, adopted by the Italian Ministry of University and Research, CUP: F83C22000720001, Spoke 14 “Hydrogen and New Fuels”].

References

[1] International Air Transport Association. Resolution on the industry’s commitment to reach net zero carbon emissions by 2050. Press Release No: 66; 2021 n.d.
[2] International Civil Aviation Organization. Resolution A41–21.: Consolidated statement of continuing ICAO policies and practices related to environmental protection - Climate change. Montreal; 2022. n.d.
[3] V. Grewe, A. Gangoli Rao, T. Grönstedt, C. Xisto, F. Linke, J. Melkert, et al., Evaluating the climate impact of aviation emission scenarios towards the Paris agreement including COVID-19 effects, Nat. Commun. 12 (1) (2021) 1–10, https://doi.org/10.1038/s41467-021-24091-y.
[4] Reducing emissions from aviation - European Commission, n.d. 〈https://climate.ec.europa.eu/eu-action/transport/reducing-emissions-aviation_en〉 (Accessed March 11, 2025).
[5] Aviation - IEA n.d. 〈https://www.iea.org/energy-system/transport/aviation〉 (Accessed March 11, 2025).
[6] CO_2 to methanol | Johnson Matthey, n.d. 〈https://matthey.com/products-and-markets/chemicals/methanol/co2-to-methanol?gad_source=1&gclid=CjwKCAjwvr–BhB5EiwAd5YbXvSSYlv-EBZ5dU44VJ_hYwIaHNWXI_J8XWM_NV2guTFO916WL3rjVhoCaogQAvD_BwE〉 (Accessed March 11, 2025).
[7] Renewable Methanol | Methanol Institute, n.d. 〈https://www.methanol.org/renewable/〉 (Accessed March 11, 2025).
[8] The world’s largest green methanol plant fuels green shipping and industry, n.d. 〈https://stateofgreen.com/en/solutions/the-worlds-largest-green-methanol-plant-fuels-green-shipping-and-industry/〉 (Accessed March 11, 2025).
[9] G. Cican, R. Mirea, G. Rimbu, Experimental evaluation of methanol/Jet-A blends as sustainable aviation fuels for turbo-engines: performance and environmental impact analysis, 2024;7:155, Fire 7 (2024) 155, https://doi.org/10.3390/FIRE7050155.
[10] The Development of Improved Fuel Specifications for Methanol (M85) and Ethanol (E d 85) on JSTOR, n.d. 〈https://www.jstor.org/stable/44612349?seq=1〉 (Accessed March 17, 2025).
[11] AMF, n.d. 〈https://iea-amf.org/content/fuel_information/methanol〉 (Accessed March 17, 2025).
[12] Safe Handling | Methanol Institute, n.d. 〈https://www.methanol.org/safe-handling/〉 (Accessed March 17, 2025).
[13] Methanol Takes Lead in Shipping’s Quest for Green Fuel - WSJ, n.d. 〈https://www.wsj.com/articles/methanol-shipping-green-fuel-11675445221〉 (Accessed March 17, 2025).
[14] Methanol as fuel heads for the mainstream in shipping, n.d. 〈https://www.dnv.com/expert-story/maritime-impact/Methanol-as-fuel-heads-for-the-mainstream-in-shipping/〉 (Accessed March 17, 2025).
[15] P.C. Shukla, G. Belgiorno, G. Di Blasio, A.K. Agarwal, editors. Alcohol as an Alternative Fuel for Internal Combustion Engines, 2021. 〈https://doi.org/10.1007/978-981-16-0931-2〉.
[16] Who we are | About us | ExxonMobil, n.d. 〈https://corporate.exxonmobil.com/who-we-are#Exploremore〉 (Accessed March 11, 2025).
[17] Topsoe, n.d. 〈https://www.topsoe.com/〉 (Accessed March 11, 2025).
[18] Verde, n.d. 〈https://www.verdecleanfuels.com/〉 (Accessed March 11, 2025).
[19] CARBON CAPTURE HONEYWELL UOP eFINING TM UOP eFINING ENABLES HIGHLY SELECTIVE, LOW CARBON INTENSITY PRODUCTION OF SAF FROM CO2 OR SYNGAS FOR eFUEL PROFITABILITY, 2023.

[20] Vertimass – Developing breakthrough biofuel technologies, n.d. 〈https://www.vertimass.com/〉 (Accessed March 11, 2025).
[21] C. Streck, P. Keenlyside, M. Von Unger, The Paris agreement: a new beginning, J. Eur. Environ. Plan. Law 13 (2016) 3–29, https://doi.org/10.1163/18760104-01301002.
[22] P. Schmidt, V. Batteiger, A. Roth, W. Weindorf, T. Raksha, Power-to-liquids as renewable fuel option for aviation: a review, Chem. Ing. Tech. 90 (2018) 127–140, https://doi.org/10.1002/CITE.201700129.
[23] R.C. Baliban, J.A. Elia, C.A. Floudas, Biomass to liquid transportation fuels (BTL) systems: process synthesis and global optimization framework, Energy Environ. Sci. 6 (2012) 267–287, https://doi.org/10.1039/C2EE23369J.
[24] V.I. Erofeev, I.S. Khomyakov, L.A. Egorova, Production of high-octane gasoline from straight-run gasoline on ZSM-5 modified zeolites, Theor. Found. Chem. Eng. 48 (2014) 71–76, https://doi.org/10.1134/S0040579514010023/METRICS.
[25] H. Song, N. Wang, H.L. Song, F. Li, La–Ni modified S2O82 – /ZrO2-Al2O3 catalyst in n-pentane hydroisomerization, Catal. Commun. 59 (2015) 61–64, https://doi.org/10.1016/J.CATCOM.2014.09.037.
[26] A. Galadima, R.P.K. Wells, J.A. Anderson, n-Alkane hydroconversion over carbided molybdena supported on sulfated zirconia, 1 2011;1, Appl. Petrochem. Res. 1 (2011) 35–43, https://doi.org/10.1007/S13203-011-0004-0.
[27] J. Ou, H. Guo, J. Zheng, K. Cheung, P.K.K. Louie, Z. Ling, et al., Concentrations and sources of non-methane hydrocarbons (NMHCs) from 2005 to 2013 in Hong Kong: a multi-year real-time data analysis, Atmos. Environ. 103 (2015) 196–206, https://doi.org/10.1016/J.ATMOSENV.2014.12.048.
[28] A.K. Agarwal, T. Gupta, P. Bothra, P.C. Shukla, Emission profiling of diesel and gasoline cars at a city traffic junction, Particuology 18 (2015) 186–193, https://doi.org/10.1016/J.PARTIC.2014.06.008.
[29] N.A. Owen, O.R. Inderwildi, D.A. King, The status of conventional world oil reserves—hype or cause for concern? Energy Policy 38 (2010) 4743–4749, https://doi.org/10.1016/J.ENPOL.2010.02.026.
[30] C.J. Campbell, J.H. Laherrère, The End of Cheap Oil, 1998;278:78–83. https://doi.org/10.2307/26057708.
[31] J.D. Edwards, Crude oil and alternate energy production forecasts for the twenty-first century: the end of the hydrocarbon era, Am. Assoc. Pet. Geol. Bull. 81 (1997) 1292–1305, https://doi.org/10.1306/522B4DE3-1727-11D7-8645000102C1865D.
[32] S. Yurchak, Development of mobil's fixed-bed methanul-to-gasoline (MTG) process, Stud. Surf. Sci. Catal. 36 (1988) 251–272, https://doi.org/10.1016/S0167-2991(09)60521-8.
[33] D.M. Marcus, K.A. McLachlan, M.A. Wildman, J.O. Ehresmann, P.W. Kletnieks, J.F. Haw, Experimental evidence from H/D exchange studies for the failure of direct C–C coupling mechanisms in the methanol-to-olefin process catalyzed by HSAPO-34, Angew. Chem. Int. Ed. 45 (2006) 3133–3136, https://doi.org/10.1002/ANIE.200504372.
[34] C.M. Wang, Y.D. Wang, Z.K. Xie, Insights into the reaction mechanism of methanol-to-olefins conversion in HSAPO-34 from first principles: are olefins themselves the dominating hydrocarbon pool species? J. Catal. 301 (2013) 8–19, https://doi.org/10.1016/J.JCAT.2013.01.024.
[35] E. Kianfar, S. Hajimirzaee, S. mousavian, A.S. Mehr, Zeolite-based catalysts for methanol to gasoline process: a review, Microchem. J. 156 (2020) 104822, https://doi.org/10.1016/J.MICROC.2020.104822.
[36] G. Luo, A.G. McDonald, Conversion of methanol and glycerol into gasoline via ZSM-5 catalysis, Energy Fuels 28 (2014) 600–606, https://doi.org/10.1021/EF401993X/ASSET/IMAGES/LARGE/EF-2013-01993X_0010.JPEG.
[37] A.T. Aguayo, A.G. Gayubo, M. Castilla, J.M. Arandes, M. Olazar, J. Bilbao, MTG process in a fixed-bed reactor. Operation and simulation of a pseudoadiabatic experimental unit, Ind. Eng. Chem. Res 40 (2001) 6087–6098, https://doi.org/10.1021/IE0101893/ASSET/IMAGES/LARGE/IE0101893F00017.JPEG.
[38] A. Galadima, O. Muraza, From synthesis gas production to methanol synthesis and potential upgrade to gasoline range hydrocarbons: a review, J. Nat. Gas. Sci. Eng. 25 (2015) 303–316, https://doi.org/10.1016/J.JNGSE.2015.05.012.
[39] M. Iglesias Gonzalez, B. Kraushaar-Czarnetzki, G. Schaub, Process comparison of biomass-to-liquid (BtL) routes Fischer-Tropsch synthesis and methanol to gasoline, Biomass. Convers. Biorefin 1 (2011) 229–243, https://doi.org/10.1007/S13399-011-0022-2/TABLES/18.
[40] M. Stöcker, Methanol-to-hydrocarbons: catalytic materials and their behavior, Microporous Mesoporous Mater. 29 (1999) 3–48, https://doi.org/10.1016/S1387-1811(98)00319-9.
[41] Research E. Coal to Clean gasoline. n.d.
[42] NETL, 2014. U.S. Department of Energy; Liquid Fuels, Conversion of Methanol to Gasoline. National Energy Technology Laboratory, United State of America. n.d.
[43] J. Topp-Jørgensen, Topsøe integrated gasoline synthesis – the tigas process, Stud. Surf. Sci. Catal. 36 (1988) 293–305, https://doi.org/10.1016/S0167-2991(09)60523-1.
[44] C. Colella, Zeolites and ordered mesoporous materials: progress and prospects, Stud. Surf. Sci. Catal. 157 (2005) 13–40.
[45] B.M. Abu-Zied, W. Schwieger, A. Unger, Nitrous oxide decomposition over transition metal exchanged ZSM-5 zeolites prepared by the solid-state ion-exchange method, Appl. Catal. B 84 (2008) 277–288, https://doi.org/10.1016/J.APCATB.2008.04.004.
[46] L. Shirazi, E. Jamshidi, M.R. Ghasemi, The effect of Si/Al ratio of ZSM-5 zeolite on its morphology, acidity and crystal size, Cryst. Res. Technol. 43 (2008) 1300–1306, https://doi.org/10.1002/CRAT.200800149.
[47] D.M. Bibby, R.F. Howe, G.D. McLellan, Coke formation in high-silica zeolites, Appl. Catal. A Gen. 93 (1992) 1–34, https://doi.org/10.1016/0926-860X(92)80291-J.
[48] Y. Gao, B. Zheng, G. Wu, F. Ma, C. Liu, Effect of the Si/Al ratio on the performance of hierarchical ZSM-5 zeolites for methanol aromatization, RSC Adv. 6 (2016) 83581–83588, https://doi.org/10.1039/C6RA17084F.
[49] K. Wang, M. Dong, X. Niu, J. Li, Z. Qin, W. Fan, et al., Highly active and stable Zn/ZSM-5 zeolite catalyst for the conversion of methanol to aromatics: effect of support morphology, Catal. Sci. Technol. 8 (2018) 5646–5656, https://doi.org/10.1039/C8CY01734D.
[50] F.L. Bleken, K. Barbera, F. Bonino, U. Olsbye, K.P. Lillerud, S. Bordiga, et al., Catalyst deactivation by coke formation in microporous and desilicated zeolite H-ZSM-5 during the conversion of methanol to hydrocarbons, J. Catal. 307 (2013) 62–73, https://doi.org/10.1016/J.JCAT.2013.07.004.
[51] G.V. Echevskii, K.G. Ione, G.N. Nosyreva, G.S. Litvak, Effect of the temperature regime of methanol conversion to hydrocarbons on coking of zeolite catalysts and their regeneration, Appl. Catal. 43 (1988) 85–89, https://doi.org/10.1016/S0166-9834(00)80902-1.
[52] C.D. Chang, J.C.W. Kuo, W.H. Lang, S.M. Jacob, J.J. Wise, A.J. Silvestrl, Process studies on the conversion of methanol to gasoline, Ind. Eng. Chem. Process Des. Dev. 17 (1978) 255–260, https://doi.org/10.1021/I260067A008.
[53] H.A. Zaidi, K.K. Pant, Catalytic conversion of methanol to gasoline range hydrocarbons, Catal. Today 96 (2004) 155–160, https://doi.org/10.1016/J.CATTOD.2004.06.123.
[54] M. Bjørgen, F. Joensen, M. Spangsberg Holm, U. Olsbye, K.P. Lillerud, S. Svelle, Methanol to gasoline over zeolite H-ZSM-5: improved catalyst performance by treatment with NaOH, Appl. Catal. A Gen. 345 (2008) 43–50, https://doi.org/10.1016/J.APCATA.2008.04.020.
[55] A. Sanz-Martínez, J. Lasobras, J. Soler, J. Herguido, M. Menéndez, Methanol to gasoline (MTG): parametric study and validation of the process in a two-zone fluidized bed reactor (TZFBR), J. Ind. Eng. Chem. 113 (2022) 189–195, https://doi.org/10.1016/J.JIEC.2022.05.045.
[56] Z. Wan, G. Li, C. Wang, H. Yang, D. Zhang, Effect of reaction conditions on methanol to gasoline conversion over nanocrystal ZSM-5 zeolite, Catal. Today 314 (2018) 107–113, https://doi.org/10.1016/J.CATTOD.2018.01.017.
[57] C. Arias Gallego, M. Khandavilli, L. Kobayashi, S.M. Sarathy, Kinetic modeling and techno-economic analysis of a methanol-to-gasoline production repurposed refinery equipment, ACS Omega 9 (2024) 22858–22870, https://doi.org/10.1021/ACSOMEGA.4C01327/ASSET/IMAGES/LARGE/AO4C01327_0017.JPEG.
[58] S.D. Phillips, J.K. Tarud, M.J. Biddy, A. Dutta, Gasoline from Wood via Integrated Gasification, Synthesis, and Methanol-to-Gasoline Technologies 2011. https://doi.org/10.2172/1004790.
[59] M. Hennig, technology MH-F processing, 2021 undefined. Techno-economic analysis of hydrogen enhanced methanol to gasoline process from biomass-derived synthesis gas. ElsevierM Hennig, M HaaseFuel Processing Technology, 2021•Elsevier n.d.
[60] D.E. Krohn, M.G. Melconian, The first fixed-bed methanol-to-gasoline (MTG) plant: design and scale-up considerations, Stud. Surf. Sci. Catal. 36 (1988) 679–689, https://doi.org/10.1016/S0167-2991(09)60565-6.
[61] O. Rojas, Dimethyl ether as building block for the production of green fuels, 2018.
[62] M. E-Moghaddam, N. Dahmen, U. Santo, J. Sauer, Gasoline synthesis from biomass-derived syngas comparing different methanol and dimethyl ether pathways by process simulation, based on the bioliq process, Energy Fuels 38 (2024) 4229–4243, https://doi.org/10.1021/acs.energyfuels.3c04524.
[63] G. Liu, E.D. Larson, Comparison of coal/biomass co-processing systems with CCS for production of low-carbon synthetic fuels: methanol-to-gasoline and Fischer-Tropsch, Energy Procedia 63 (2014) 7315–7329, https://doi.org/10.1016/j.egypro.2014.11.768 Elsevier Ltd.
[64] C.D. Chang, A.J. Silvestri, The conversion of methanol and other O-compounds to hydrocarbons over zeolite catalysts, J. Catal. 47 (1977) 249–259, https://doi.org/10.1016/0021-9517(77)90172-5.
[65] TRIPPE FREDERIK. TECHNO-OEKONOMISCHE BEWERTUNG ALTERNATIVER VERFAHRENSKONFIGURATIONEN ZUR HERSTELLUNG VON… BIOMASS-TO-LIQUID (BTL) KRAFTSTOFFEN UND CHEMIKALI 2014.
[66] J. Choe, C. Choe, T. Kim, Y. Pak, C. Han, H. Yun, Novel kinetic modelling of methanol-to-gasoline (MTG) reaction on HZSM-5 catalyst: product distribution, J. Indian Chem. Soc. 98 (2021) 100003, https://doi.org/10.1016/J.JICS.2021.100003.
[67] C.D. Chang, Hydrocarbons from methanol, Catal. Rev. Sci. Eng. 25 (1983) 1–118, https://doi.org/10.1080/01614948308078874.
[68] A.W. Chester, Y.F. Chu, Treatment of effluent resulting from conversion of methanol to gasoline in order to decrease durene and produce distillate, 1982.
[69] H. Vivas, F. Joensen, Process and catalyst for upgrading gasoline, 2013.
[70] J. Ruokonen, H. Nieminen, A.R. Dahiru, A. Laari, T. Koiranen, P. Laaksonen, et al., Modelling and cost estimation for conversion of green methanol to renewable liquid transport fuels via olefin oligomerisation, Processes 9 (2021) 1046, https://doi.org/10.3390/PR9061046/S1.
[71] M.F. Wilson, I.P. Fisher, J.F. Kriz, Hydrogenation and extraction of aromatics from oil sands distillates and effects on cetane improvement, Energy Fuels 1 (1987) 540–544, https://doi.org/10.1021/EF00006A015.
[72] D.M. Bibby, R.F. Howe, G.D. McLellan, Coke formation in high-silica zeolites, Appl. Catal. A Gen. 93 (1992) 1–34, https://doi.org/10.1016/0926-860X(92)80291-J.
[73] J. MacDonald, D. Lopez-Pintor, N. Matsubara, K. Kitano, R. Yamada, A chemical kinetic analysis of knock propensity of methanol-to-gasoline fuel, Fuel 382 (2025) 133787, https://doi.org/10.1016/J.FUEL.2024.133787.
[74] F.L. Bleken, K. Barbera, F. Bonino, U. Olsbye, K.P. Lillerud, S. Bordiga, et al., Catalyst deactivation by coke formation in microporous and desilicated zeolite H-ZSM-5 during the conversion of methanol to hydrocarbons, J. Catal. 307 (2013) 62–73, https://doi.org/10.1016/J.JCAT.2013.07.004.

[75] A. Palizdar, A. Vatani, Methanol to gasoline process: design and analysis of a structure with the minimum energy requirement and proposal of a novel integrated configuration to improve profitability, Energy 316 (2025) 134459, https://doi.org/10.1016/j.energy.2025.134459.
[76] S. Liu, J. He, D. Lu, J. Sun, Optimal integration of methanol-to-gasoline process with organic Rankine cycle, Chem. Eng. Res. Des. 154 (2020) 182–191, https://doi.org/10.1016/j.cherd.2019.11.036.
[77] S.A. Tabak, A.A. Avidan, F.J. Krambeck, Production of synthetic gasoline and diesel fuel from nonpetroleum resources, Am. Chem. Soc. Div. Gas. Fuel Chem. Prepr. 31 (1986) 2.
[78] A.A. Avidan, Gasoline and distillate fuels from methanol, Stud. Surf. Sci. Catal. 36 (1988) 307–323, https://doi.org/10.1016/S0167-2991(09)60524-3.
[79] M. Stöcker, Methanol-to-hydrocarbons: catalytic materials and their behavior, Microporous Mesoporous Mater. 29 (1999) 3–48, https://doi.org/10.1016/S1387-1811(98)00319-9.
[80] P. Schmidt, W. Zittel, W. Weindorf, T. Rakasha, D. Goericke, Renewables in transport 2050 – Empowering a sustainable mobility future with zero emission fuels, 2016. pp. 185–199. https://doi.org/10.1007/978-3-658-13255-2_15.
[81] I.M. Dahl, S. Kolboe, On the reaction mechanism for hydrocarbon formation from methanol over SAPO-34: I. Isotopic labeling studies of the Co-reaction of ethene and methanol, J. Catal. 149 (1994) 458–464, https://doi.org/10.1006/JCAT.1994.1312.
[82] S.A. Tabak, S. Yurchak, Conversion of methanol over ZSM-5 to fuels and chemicals, Catal. Today 6 (1990) 307–327, https://doi.org/10.1016/0920-5861(90)85007-B.
[83] S. Calnan, F. Müller-Langer, N. Beltermann, R. Peters, R. Can Samsun, Closing the gap between sustainable aviation fuels and fossil aviation fuels. Resiliente Lieferketten Und Rohstoffversorgung, Sustain. Aviat. Fuels (2023) 19–25.
[84] I.M. Dahl, S. Kolboe, On the reaction mechanism for hydrocarbon formation from methanol over SAPO-34: I. Isotopic labeling studies of the co-reaction of ethene and methanol, J. Catal. 149 (1994) 458–464, https://doi.org/10.1006/JCAT.1994.1312.
[85] H. Olivier-Bourbigou, P.A.R. Breuil, L. Magna, T. Michel, M.F. Espada Pastor, D. Delcroix, Nickel catalyzed olefin oligomerization and dimerization, Chem. Rev. 120 (2020) 7919–7983, https://doi.org/10.1021/ACS.CHEMREV.0C00076/ASSET/IMAGES/MEDIUM/CR0C00076_0041.GIF.
[86] A. Corma, MA, M-S V, Innovative catalytic processes for the conversion of methanol into hydrocarbons in the gasoline and middle distillate range, Catal. Today 38 (4) (1997) 305–318.
[87] J. Weitkamp, Catalytic hydrocracking—mechanisms and versatility of the process, ChemCatChem 4 (2012) 292–306, https://doi.org/10.1002/CCTC.201100315.
[88] P. Schmidt, V. Batteiger, A. Roth, W. Weindorf, T. Raksha, Power-to-liquids as renewable fuel option for aviation: a review, Chem. Ing. Tech. 90 (2018) 127–140, https://doi.org/10.1002/CITE.201700129.
[89] S. Voß, S. Bube, M. Kaltschmitt, Aviation fuel production pathways from lignocellulosic biomass via alcohol intermediates – a technical analysis, Fuel Commun. 17 (2023) 100093, https://doi.org/10.1016/J.JFUECO.2023.100093.
[90] R. Zhou, M. Jin, Z. Li, Y. Xiao, D. McCollum, A. Li, Techno-economic analysis and network design for CO_2 conversion to jet fuels in the United States, Renew. Sustain. Energy Rev. 210 (2025) 115191, https://doi.org/10.1016/J.RSER.2024.115191.
[91] J. Weitkamp, Zeolites and catalysis, Solid State Ion. 131 (2000) 175–188, https://doi.org/10.1016/S0167-2738(00)00632-9.
[92] S. Voß, S. Bube, M. Kaltschmitt, Hybrid biomass- and electricity-based kerosene production—a techno-economic analysis, Energy Fuels 38 (2024) 5263–5278, https://doi.org/10.1021/ACS.ENERGYFUELS.3C04876/ASSET/IMAGES/LARGE/EF3C04876_0014.JPEG.
[93] B. Wang, Z.J. Ting, M. Zhao, Sustainable aviation fuels: key opportunities and challenges in lowering carbon emissions for aviation industry, Carbon Capture Sci. Technol. 13 (2024) 100263, https://doi.org/10.1016/J.CCST.2024.100263.
[94] S. Zoller, E. Koepf, D. Nizamian, M. Stephan, A. Patané, P. Haueter, et al., A solar tower fuel plant for the thermochemical production of kerosene from H2O and CO2, Joule 6 (2022) 1606–1616, https://doi.org/10.1016/j.joule.2022.06.012.
[95] H. Singh, C. Li, P. Cheng, X. Wang, Q. Liu, A critical review of technologies, costs, and projects for production of carbon-neutral liquid e-fuels from hydrogen and captured CO 2, Energy Adv. 1 (2022) 580–605, https://doi.org/10.1039/D2YA00173J.
[96] S. Bube, S. Voß, G. Quante, M. Kaltschmitt, Cost analysis of kerosene production from power-based syngas via the Fischer-Tropsch and methanol pathway, Fuel 384 (2025) 133901, https://doi.org/10.1016/j.fuel.2024.133901.
[97] J. Ruokonen, H. Nieminen, A.R. Dahiru, A. Laari, T. Koiranen, P. Laaksonen, et al., Modelling and cost estimation for conversion of green methanol to renewable liquid transport fuels via olefin oligomerisation, Processes 9 (2021) 1046, https://doi.org/10.3390/pr9061046.
[98] K. Atsonios, J. Li, V.J. Inglezakis, Process analysis and comparative assessment of advanced thermochemical pathways for e-kerosene production, Energy 278 (2023) 127868, https://doi.org/10.1016/J.ENERGY.2023.127868.
[99] V. Dieterich, A. Buttler, A. Hanel, H. Spliethoff, S. Fendt, Power-to-liquid via synthesis of methanol, DME or Fischer–Tropsch-fuels: a review, Energy Environ. Sci. 13 (2020) 3207–3252, https://doi.org/10.1039/D0EE01187H.
[100] S. Bube, N. Bullerdiek, S. Voß, M. Kaltschmitt, Kerosene production from power-based syngas – a technical comparison of the Fischer-Tropsch and methanol pathway, Fuel 366 (2024) 131269, https://doi.org/10.1016/J.FUEL.2024.131269.
[101] V. Eyberg, V. Dieterich, S. Bastek, M. Dossow, H. Spliethoff, S. Fendt, Techno-economic assessment and comparison of Fischer–Tropsch and methanol-to-jet processes to produce sustainable aviation fuel via Power-to-Liquid, Energy Convers. Manag 315 (2024) 118728, https://doi.org/10.1016/J.ENCONMAN.2024.118728.
[102] L. Colelli, V. Segneri, C. Bassano, G. Vilardi, E-fuels, technical and economic analysis of the production of synthetic kerosene precursor as sustainable aviation fuel, Energy Convers. Manag 288 (2023) 117165, https://doi.org/10.1016/J.ENCONMAN.2023.117165.
[103] M.F. Rojas-Michaga, S. Michailos, E. Cardozo, M. Akram, K.J. Hughes, D. Ingham, et al., Sustainable aviation fuel (SAF) production through power-to-liquid (PtL): a combined techno-economic and life cycle assessment, Energy Convers. Manag 292 (2023) 117427, https://doi.org/10.1016/J.ENCONMAN.2023.117427.
[104] A. Schaadt, Perspectives on Methanol to Jet Fuel-SAFari Project-aireg Webinar on Sustainable Aviation, 6.11.24 n.d.
[105] C.R. Ranucci, H.J. Alves, M.R. Monteiro, C.L. Kugelmeier, R.A. Baricatti, C. Rodrigues de Oliveira, et al., Potential alternative aviation fuel from jatropha (Jatropha curcas L.), babassu (Orbignya phalerata) and palm kernel (Elaeis guineensis) as blends with Jet-A1 kerosene, J. Clean. Prod. 185 (2018) 860–869, https://doi.org/10.1016/J.JCLEPRO.2018.03.084.
[106] E.D. Metzger, C.K. Brozek, R.J. Comito, M. Dinca, Selective dimerization of ethylene to 1-butene with a porous catalyst, ACS Cent. Sci. 2 (2016) 148–153, https://doi.org/10.1021/ACSCENTSCI.6B00012/ASSET/IMAGES/LARGE/OC-2016-00012P_0003.JPEG.
[107] X. Li, D. Han, H. Wang, G. Liu, B. Wang, Z. Li, et al., Propene oligomerization to high-quality liquid fuels over Ni/HZSM-5, Fuel 144 (2015) 9–14, https://doi.org/10.1016/J.FUEL.2014.12.005.
[108] X. Zhang, J. Zhong, J. Wang, J. Gao, A. Liu, Trimerization of butene over Ni-doped zeolite catalyst: effect of textural and acidic properties, Catal. Lett. 126 (2008) 388–395, https://doi.org/10.1007/S10562-008-9642-Y/FIGURES/6.
[109] M.I. Ahmad, N. Zhang, M. Jobson, Integrated design of diesel hydrotreating processes, Chem. Eng. Res. Des. 89 (2011) 1025–1036, https://doi.org/10.1016/J.CHERD.2010.11.021.
[110] M.R. Gogate, Methanol-to-olefins process technology: current status and future prospects, Pet. Sci. Technol. 37 (2019) 559–565, https://doi.org/10.1080/10916466.2018.1555589.
[111] C. Samanta, R.K. Das, C3-based petrochemicals: recent advances in processes and catalysts, Catal. Clean. Energy Environ. Sustain. Petrochem. Refin. Process. 2 (2021) 149–204, https://doi.org/10.1007/978-3-030-65021-6_5.
[112] A.P. Ortiz-Espinoza, M.M.B. Noureldin, M.M. El-Halwagi, A. Jiménez-Gutiérrez, Design, simulation and techno-economic analysis of two processes for the conversion of shale gas to ethylene, Comput. Chem. Eng. 107 (2017) 237–246, https://doi.org/10.1016/J.COMPCHEMENG.2017.05.023.
[113] B.V. Vora, T.L. Marker, P.T. Barger, H.R. Nilsen, S. Kvisle, T. Fuglerud, Economic route for natural gas conversion to ethylene and propylene, Stud. Surf. Sci. Catal. 107 (1997) 87–98, https://doi.org/10.1016/S0167-2991(97)80321-7.
[114] A.C. Dimian, C.S. Bildea, Energy efficient methanol-to-olefins process, Chem. Eng. Res. Des. 131 (2018) 41–54, https://doi.org/10.1016/J.CHERD.2017.11.009.
[115] Molecular Characterisation and Modelling of Hydroprocesses n.d.
[116] S. Drünert, U. Neuling, T. Zitscher, M. Kaltschmitt, Power-to-Liquid fuels for aviation – processes, resources and supply potential under German conditions, Appl. Energy 277 (2020) 115578, https://doi.org/10.1016/J.APENERGY.2020.115578.
[117] J. Weitkamp, Catalytic hydrocracking—mechanisms and versatility of the process, ChemCatChem 4 (2012) 292–306, https://doi.org/10.1002/CCTC.201100315.
[118] G. Cican, R. Mirea, G. Rimbu, Experimental evaluation of methanol/jet-a blends as sustainable aviation fuels for turbo-engines: performance and environmental impact analysis, 2024;7:155, Fire 7 (2024) 155, https://doi.org/10.3390/FIRE7050155.
[119] M. Fasihi, C. Breyer, Global production potential of green methanol based on variable renewable electricity, Energy Environ. Sci. 17 (2024) 3503–3522, https://doi.org/10.1039/D3EE02951D.
[120] M.J. Bos, S.R.A. Kersten, D.W.F. Brilman, Wind power to methanol: Renewable methanol production using electricity, electrolysis of water and CO2 air capture, Appl. Energy 264 (2020) 114672, https://doi.org/10.1016/J.APENERGY.2020.114672.
[121] R. Kajaste, M. Hurme, P. Oinas, Methanol-managing greenhouse gas emissions in the production chain by optimizing the resource base, AIMS Energy 6 (2018) 1074–1102, https://doi.org/10.3934/ENERGY.2018.6.1074.
[122] S.D. Phillips, J.K. Tarud, M.J. Biddy, A. Dutta, Gasoline from woody biomass via thermochemical gasification, methanol synthesis, and methanol-to-gasoline technologies: a technoeconomic analysis, Ind. Eng. Chem. Res 50 (2011) 11734–11745, https://doi.org/10.1021/IE2010675/ASSET/IMAGES/LARGE/IE-2011-010675_0006.JPEG.
[123] A.M. Peters, K. Timmerhaus, R.E. West, Title Plant Design and Economics for Chemical Engineers Specific Course Information 1995;1.
[124] R.C. Baliban, J.A. Elia, V. Weekman, C.A. Floudas, Process synthesis of hybrid coal, biomass, and natural gas to liquids via Fischer–Tropsch synthesis, ZSM-5 catalytic conversion, methanol synthesis, methanol-to-gasoline, and methanol-to-olefins/distillate technologies, Comput. Chem. Eng. 47 (2012) 29–56, https://doi.org/10.1016/J.COMPCHEMENG.2012.06.032.
[125] Deactivation of Hydroprocessing Catalysts | TU Delft Repository, n.d. 〈https://repository.tudelft.nl/record/uuid:1f5f31e7-b83a-4b49-b622-bb461ae19d30〉 (Accessed February 27, 2025).